



## **NASA Electronic Parts and Package Program**

### **Physical and Electrical Characterization of Aluminum Polymer Capacitors**

**Report of FY 2009**

**NEPP Task 390-004**

**David (Donhang) Liu  
MEI Technologies Inc.  
NASA Goddard Space Flight Center  
8800 Greenbelt Road  
Greenbelt, MD 20771**

This research described in this report was carried out at Goddard Space Flight Center, under a contract with National Aeronautics and Space administration.

## Abstract

Conductive polymer aluminum capacitor (PA capacitor) is an evolution of traditional wet electrolyte aluminum capacitors by replacing liquid electrolyte with a solid, highly conductive polymer. On the other hand, the cathode construction in polymer aluminum capacitors with coating of carbon and silver epoxy for terminal connection is more like a combination of the technique that solid tantalum capacitor utilizes. This evolution and combination result in the development of several competing capacitor construction technologies in manufacturing polymer aluminum capacitors.

The driving force of this research on characterization of polymer aluminum capacitors is the rapid progress in IC technology. With the microprocessor speeds exceeding a gigahertz and CPU current demands of 80 amps and more, the demand for capacitors with higher peak current and faster repetition rates bring conducting polymer capacitors to the center of focus. This is because this type of capacitors has been known for its ultra-low ESR and high capacitance.

Polymer aluminum capacitors from several manufacturers with various combinations of capacitance, rated voltage, and ESR values were obtained and tested. The construction analysis of the capacitors revealed three different constructions: conventional rolled foil, the multilayer stacking V-shape, and a dual-layer sandwich structure. The capacitor structure and its impact on the electrical characteristics has been revealed and evaluated.

A destructive test with massive current over stress to fail the polymer aluminum capacitors reveals that all polymer aluminum capacitors failed in a benign mode without ignition, combustion, or any other catastrophic failures.

The extraordinary low ESR (as low as 3 m $\Omega$ ), superior frequency independence reported for polymer aluminum capacitors have been confirmed. For the applications of polymer aluminum capacitors in space programs, a thermal vacuum cycle test was performed. The results, as expected, show no impact on the electrical characteristics of the capacitors.

The breakdown voltage of polymer capacitors has been evaluated using a steady step surge test. Initial results show the uniform distribution in the breakdown voltage for polymer aluminum capacitors.

Polymer aluminum capacitors with a combination of very high capacitance, extraordinary low ESR, excellent frequency stability, and non-ignite benign failure mode make it a *niche* fit in space applications for both today and future. Polymer capacitors are apparently also the best substitutes of the currently used MnO<sub>2</sub>-based tantalum capacitors in the low voltage range.

However, some critical aspects are still to be addressed in the next phase of the investigation for PA capacitors. These include the long term reliability test of 125°C dry life and 85°C/85%RH humidity, the failure mechanism and de-rating, the radiation tolerance, and the high temperature performance. All of the above requires the continuous NEPP funding and support.

## Table of Contents

<b>Introduction</b>	<b>4</b>
<b>New Challenges for Capacitor Applications</b>	<b>8</b>
1. <u>General Applications of Capacitors</u>	8
a. <i>Power Backup</i>	8
b. <i>Bypass and Decoupling</i>	9
c. <i>Filtering</i>	9
2. <u>Why Polymer Capacitors</u>	10
a. <i>Lower ESR and Improved High Frequency Performance</i>	10
b. <i>Footprint Saving and Units Miniaturization</i>	13
c. <i>Benign Failure Mode</i>	13
<b>Construction and Failure Modes of Polymer Aluminum Capacitors</b>	<b>14</b>
1. <u>Selection, Preparation, and Initial Electrical Characterization of Polymer Capacitors</u>	14
2. <u>Constructional Characterization of Polymer Aluminum Capacitors</u>	20
3. <u>Failure Modes in Aluminum Polymer Capacitors</u>	26
<b>Electrical Characterization in Frequency and Temperature Domain</b>	<b>28</b>
<b>Thermal Vacuum Testing of Aluminum Polymer Capacitors</b>	<b>34</b>
<b>Steady Step Surge Test of Aluminum Polymer Capacitors</b>	<b>36</b>
<b>Conclusions and Future Work</b>	<b>40</b>
<b>Appendix: Qualification plan for PA capacitors (Draft)</b>	<b>41</b>

## Introduction

This report summarizes the first year (FY09) physical and electrical characterization of conducting polymer based aluminum capacitors (PA capacitor).

PA capacitor is a solid electrolyte capacitor. Of the various types of electrolytic capacitors, there are primarily two types which use an electrolyte: aluminum electrolytic capacitors and tantalum electrolytic capacitors. According to the type of electrolyte used, the electrolyte capacitors can further divide into two groups: liquid (wet) electrolyte and solid electrolyte.

The application of wet aluminum electrolyte capacitors can be traced back to the early 1920s. Wet-electrolyte aluminum capacitors provided substantially more capacitance per unit volume than any other capacitor technologies of the time. The conventional construction of wet aluminum electrolyte capacitors starts with the use of a rolled oxidized aluminum foil (anode), blanketed with an absorbent spacer soaked with the electrolyte liquid, then with the cathode plate and finally another separator soaked with the electrolyte liquid (Figure 1). The entire roll was placed in a metallic cylindrical package, filled with electrolyte liquid, and then sealed with organic seal to prevent the electrolyte from escaping. For high-rel applications, the package can also be hermetically sealed.

### Wet Aluminum Electrolyte Construction (Rolled Foil)

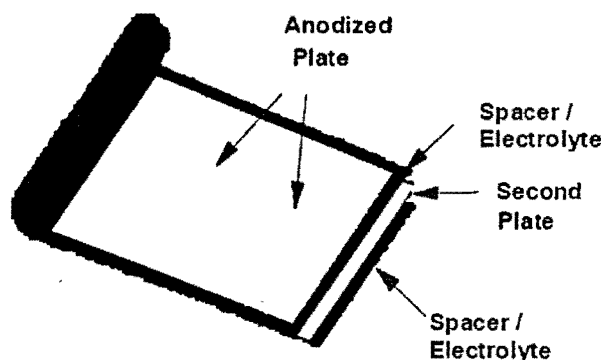


**Figure 1.** Rolled foil construction of wet aluminum electrolyte capacitors

When hermetically sealed, these wet aluminum capacitors showed high reliability in the applications where high capacitance and high voltage are both required. However, wet-aluminum capacitors have several big disadvantages: (1), they were dramatically bulky by today's standard; (2), the wet electrolyte becomes less conductive as temperature reduces, which limits its low temperatures applications; (3), due to wet electrolyte evaporation, the ultimate life time of a wet electrolyte aluminum capacitor is finite, predictable and a function of the electrolyte loss rate.

In the early 1950s, solid electrolyte tantalum capacitor was invented at Bell laboratory and soon developed into a dominant capacitor type utilized in 5-2000CV range due to its cost-effectiveness and better

performance over the bulky wet aluminum electrolyte capacitors. As shown in Figure 2, solid tantalum electrolytic capacitors starts with a sintered porous tantalum metal pellet on which a thin dielectric layer of tantalum oxide was formed (anode and dielectric).

The cathode for the solid tantalum is applied by dipping the pellet in manganese nitrate solution and then heated to  $\sim 270^{\circ}\text{C}$  for conversion from solution to  $\text{MnO}_2$ . The step is repeated for as many as hundreds time until a thick and continuous  $\text{MnO}_2$  layer is created as the cathode contact to the dielectric. A coating of graphite is then applied to the  $\text{MnO}_2$  layer to eliminate any interfacial resistance, followed by a final silver application to allow a low resistance connection to the outside termination.

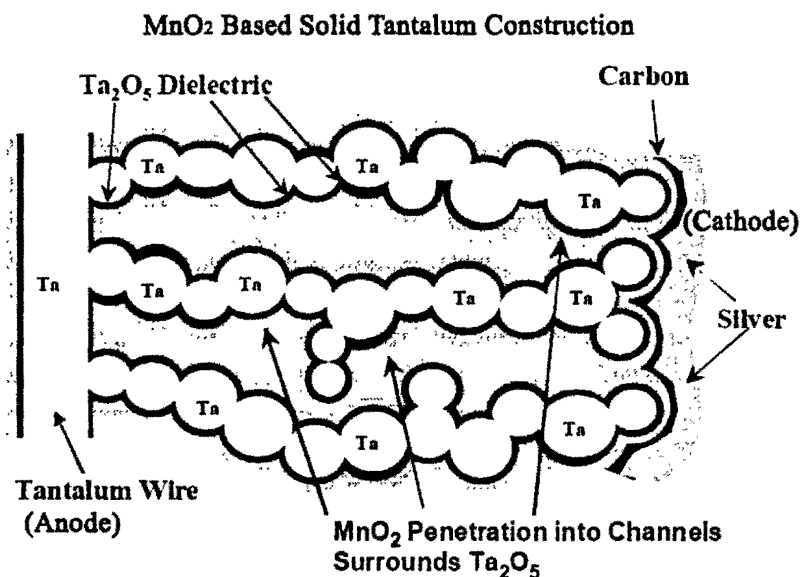


**Figure 2.** Cross-sectional illustration of solid  $\text{MnO}_2$  electrolyte tantalum construction

The  $\text{MnO}_2$  based solid electrolyte tantalum capacitors show several advantages over the wet electrolyte aluminum capacitors. First, due to the high dielectric constant and the porous structure of a tantalum pellet, tantalum capacitor has much higher capacitance per volume. This significantly reduces the size of a capacitor device and makes the surface mount possible. Second, because  $\text{MnO}_2$  is highly conductive, the capacitance loss and dissipation factor (DF) increasing with decreasing temperature is greatly minimized. Third, the replacement of solid  $\text{MnO}_2$  to liquid acidic electrolyte completely eliminates the evaporation of electrolyte, which results in a much better performance and long term reliability.

The emerging of solid tantalum capacitors meets the demand in the electronic industry for less power consumption, smaller in size, and high-density assembly such as surface mounting and thus becoming dominant since the 1970s. However, as today's IC becomes faster, and the demand for lower voltage, larger current power supply becomes stronger, the capacitors used for power backup, ripple smoothing are required to exhibit extraordinary low equivalent series resistance (ESR). Low ESR is a critical parameter for any capacitors to be used in today's high speed switching power supply and DC/DC converters.

ESR in a capacitor device is a parasitic parameter and is attributed from many factors. Tremendous research work has been done in addressing the issue. For  $\text{MnO}_2$ -based tantalum capacitors, the biggest contribution to ESR was resulted from the high resistance in  $\text{MnO}_2$  layer. The seeking on new materials with higher conductivity to replace  $\text{MnO}_2$  results in the development of conducting polymer capacitors.

In the early 1990s, a number of Japanese manufacturers were reported using highly conducting polymer materials for MnO<sub>2</sub> cathode substitution. The conducting polymer materials that exhibit processing stability and compatibility are tetracyano-quinodimethane (TCNQ), Polypyrrole (PPY), and Polyethylenedioxythiophene (PEDT, mainly for Ta polymer capacitor). All of these polymers, when processed correctly, have reported to have conductivity exceeding 100 S/cm. This is much higher conductivity than MnO<sub>2</sub>, which is generally considered to have conductivity in the neighborhood of 0.1 – 1.0 S/cm.

The conducting polymers have been applied for manufacturing both polymer tantalum capacitors and aluminum capacitors. The material change in tantalum polymer capacitors did not change the structure of the device. The polymer is a straight substitution of the MnO<sub>2</sub> in the capacitor assembly as shown in Figure 2.

On the other hand, a variety of processing changes has been made in manufacturing PA capacitors. An early version of PA capacitor processing adapted the rolled foil technique as shown in Figure 1 with a polymer material replacement of the wet electrolyte. In detail, a molten TCNQ salt was poured into the structure after the Al foils and spacers were loosely wound. The TCNQ salt filled the voids between the cathode and the dielectric layers surface as well as the etched tunnels within the anode foils structure. After solidifying the TCNQ salt at room temperature, a high conductivity layer was created between the cathode and aluminum oxide surface.

Unlike the rolled foil structure for wet electrolyte in which all foil layers can be wound together tightly, the polymer rolled foils were wound *loosely* in order to reserve a large gap to prevent the rubbing between cathode foil and anode film to cause a short circuit. This makes the rolled foil technique not a best approach for PA capacitors.

In order to overcome the large gap in rolled foil technique, a stacking foil approach as shown in Figure 3 was developed. The etched and anodized aluminum foils are stacked and bonded together into a single

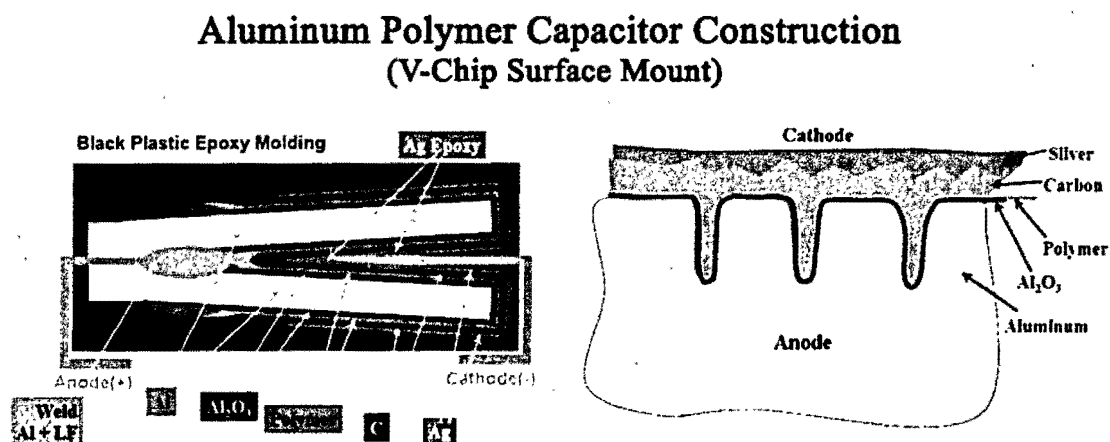


**Figure 3.** Cross-sectional illustration of aluminum polymer capacitor construction of lead frame version for surface mounting (courtesy of KEMET)

structure (it can be stacked in multiple layers). The structure is then repeatedly dipped so that the loose ends of the plates are immersed into the monomer solution. The coating polymerizes on the surface of the dielectric coating and into the etched tunnels of the anode foil plate.

Next, a coating of graphite is applied prior the silver epoxy application. Finally these stacking plates are bonded using a silver epoxy to the cathode lead frame, while the anode lead frame is welded to the bond area of aluminum plate. This design facilitates the surface mount termination and utilizes the capacitor spacing more effectively, and therefore is adapted by many manufacturers.

Although the initial driving force for the development of polymer capacitors is to reduce the ESR, the results are more compelling than ESR itself. Both tantalum and aluminum polymer capacitors also exhibit improved performance such as faster dynamic transient response, better ripple voltage smoothing, superior reliability, and open-circuit, ignition-free failure mechanism.

The characterization of tantalum polymer capacitors has been conducted thoroughly in a previous NEPP funded program by Dr. Erik Reed. In this research, only aluminum polymer capacitors will be investigated. The characterization will be focused on both capacitor structure and electrical performance. The results will be evaluated and compared to that previously report for tantalum polymer capacitors.

Finally in this report, the future work will be proposed for the next fiscal year.

## New Challenges for Capacitor Applications

### 1. General Applications of Capacitors

In order to demonstrate the application advantages of PA capacitors in today's electronic circuits, it is necessary to briefly describe the common functions and requirements of the capacitors. In general, a capacitor can be applied for following functions:

#### *a. Power Backup*

In modern electronics, almost all electronic circuitry is driven and controlled by an IC chip. All the IC chips require a power supply to function. In most cases, the load currents in IC chips are not constant and always change during the operation. As the IC speed gets faster and faster, the rapid change in IC load will cause the power supply to not be able to supply sufficient current to the IC unit on time. This results in the line voltage drop which may stop the IC operation.

As shown in Figure 4, a capacitor can be used here for a backup to mitigate the line voltage drop by playing a temporary role of power supply to discharge a backup current to the IC unit. However, a capacitor has an equivalent circuit that contains both resistance and inductance in series, called ESR and ESL respectively. These will affect a capacitor's backup function.

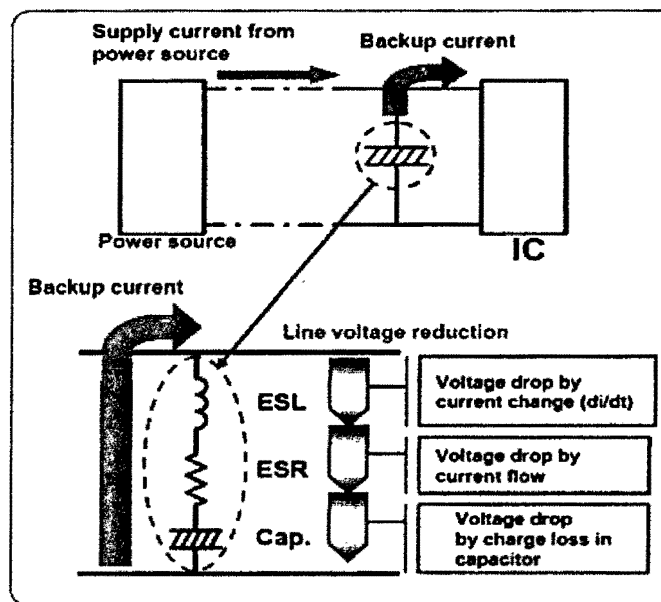


**Figure 4.** Application of capacitor as a power supply backup to an IC unit

ESR will cause a line voltage drop that is in proportion to the capacitor discharge current; ESL will cause additional line voltage drop that is in proportion to the current change with discharge time ( $ESL \approx di_d/dt$ , where  $i_d$  is the discharge current). In addition, a backup capacitor will keep discharge until the power supply unit responds to the IC load change. A capacitor with higher capacitance value will have a smaller



decrease in discharge. For this reason, the capacitors used for power backup should have large capacitance and low ESR and low ESL.

### ***b. Bypass and Decoupling***

When provides power to IC chips, a power supply will carry noises in both current and voltage through a power supply line. This will result in malfunction in IC operation. A shunt capacitor between power supply and IC unit can let AC noises from power supply bypass to the ground before reach to IC unit.

On the other hand, an IC unit in high-speed function will also generate spikes that contain harmonic current. The harmonic current may flow back to power supply and form a long loop between IC and power supply. This forms an antenna and becomes the cause of emission noise. A decoupling capacitor shunted with IC chip, as shown in Figure 5, will circulate the harmonic current in a short loop and prevent it flow back to power supply. In order to handle an ample amount of noise in both bypass and decoupling applications, the capacitor must have high capacitance and extreme low impedance (low ESR).

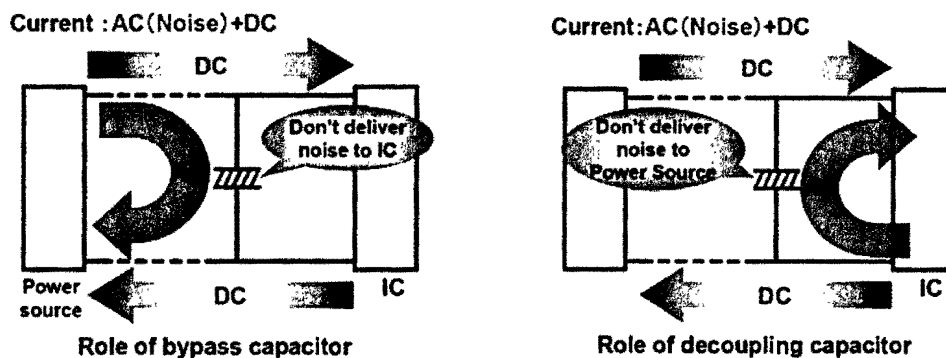


**Figure 5.** Bypass and decoupling applications of capacitors

### ***c. Filtering***

Another important application of capacitors is to form a passive filter in connection with resistor and inductors. Various filters are used to reduce switching noises in digital-analog circuits. Figure 6 shows some typical passive filters and a diagram to explain how a LC filter circuit can be designed for improved performance.

Based on the filtering transfer function, a LC filter is characterized by two frequency points called “pole”  $F_p$  and “zero point”  $F_z$ :

$$\text{Pole } F_p = \frac{1}{2\pi\sqrt{LC}} \quad \text{Zero point } F_z = \frac{1}{2\pi\sqrt{C R_{ESR}}} \quad (1)$$

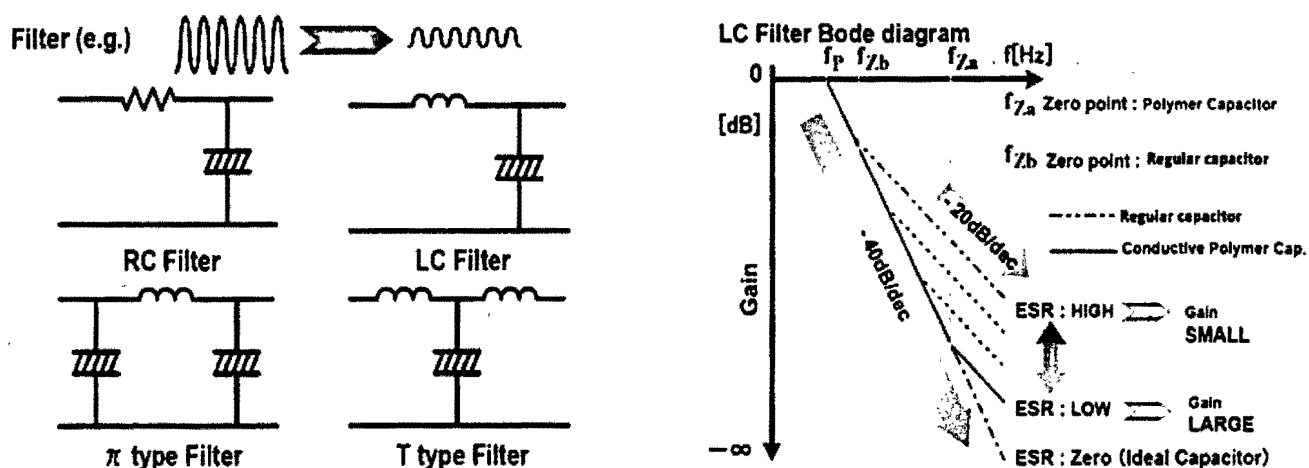


Figure 6. Filtering applications of capacitors

Where the pole is the frequency at which a gain slope equals to -40db/dec; zero point is the frequency of -20db/dec. The higher the pole and zero point, the better the noise removal characteristics in high frequencies. As shown in equation (1), it is clear that higher capacitance and lower ESR is the key for higher pole and zero point, and thus for better filtering performance at higher frequencies.

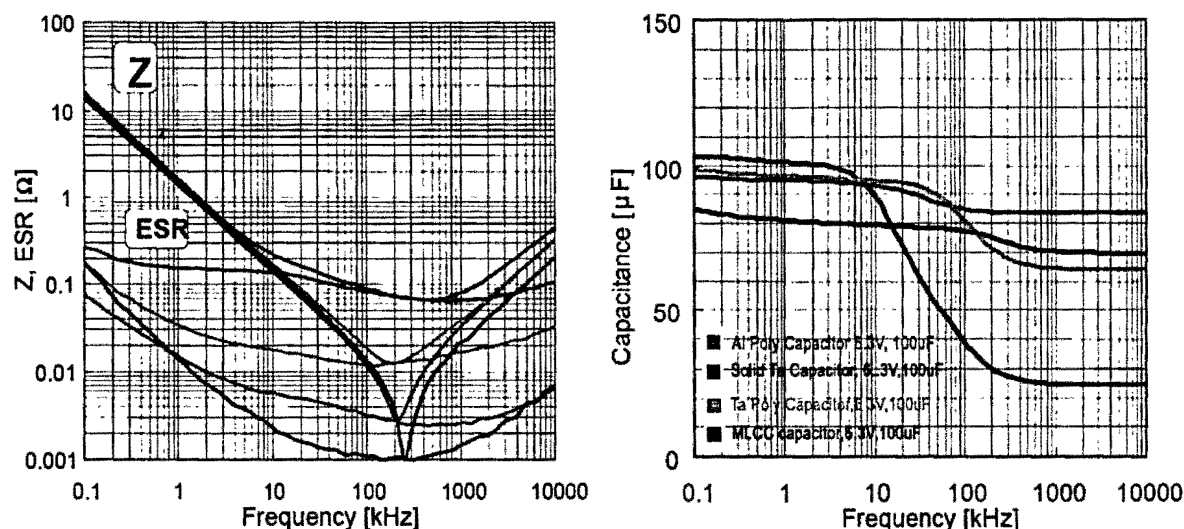
## 2. Why Polymer Capacitors

The high speed and high power usage in today's electronic circuits results in a strong demand for high capacitance and low ESR and low ESL. In comparison to solid tantalum capacitors and wet aluminum electrolyte capacitors which have been widely used for these applications, the primary reason for the need of aluminum polymer capacitors, made with conducting polymer electrolyte, is that conducting polymers are significantly more conductive than  $MnO_2$  and fluid electrolyte, perhaps up to 100 times more conductive. The direct benefits of this increased conductivity are lower ESR and improved high-frequency performance.

### a. Lower ESR and Improved High Frequency Performance

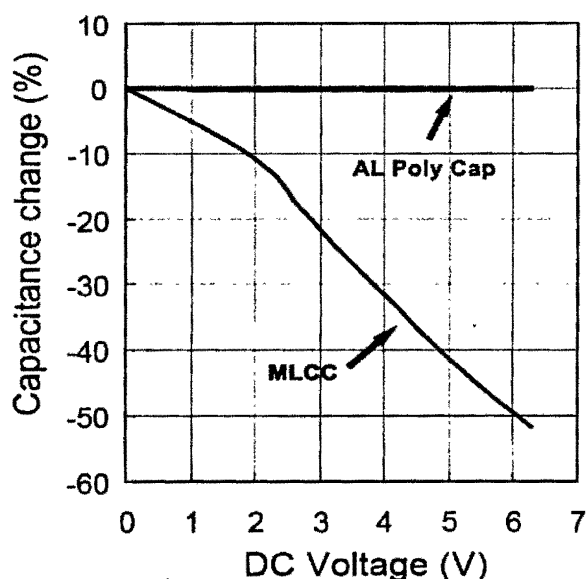
One of the immediate improvements after using high conductive polymer is the significant reduction in ESR. Almost every PA capacitor in the market today can readily reach an ESR in single digit milliohms. In addition, the conductivity of the polymers is not changed much even at extremely low temperatures. This is a big advantage in comparison to the liquid electrolyte where conductivity is reduced dramatically with temperature reduction. The direct performance improvement is the stable capacitance at high frequencies.

Figure 7 shows the comparison of frequency-domain impedance, ESR, and capacitance for four 6.3V, 100 $\mu$ F capacitors made of different materials. It clearly shows that PA capacitor exhibits almost comparable performance with multi-layer ceramic capacitors (MLCC) in both ESR and capacitance stability.



**Figure 7.** Frequency-domain characteristics of various types of capacitors (data courtesy of Panasonic)

The testing data in Figure 7 may raise some questions such as why don't we simply use MLC capacitor (MLCC) to replace all tantalum and aluminum capacitors since MLCC has the best frequency-domain performance. The answers for the questions are: First, the MLCC can not be able to achieve the same high capacitance as tantalum and aluminum capacitors for the same given footprint and volume. Secondly, the MLCC exhibits strong capacitance dependence on DC bias due to the ferroelectric dielectric materials used for MLCCs. The polymer capacitors, on the other hand, show almost no capacitance-voltage dependence (see Figure 8).



**Figure 8.** Capacitance as a function of DC bias in PA capacitor and MLCC of various types of capacitors (data courtesy of Panasonic)

Aluminum polymer capacitors show even lower ESR than tantalum polymer capacitors due to the difference in capacitor construction technologies. The aluminum polymer capacitor starts with a fine etched

and oxidized anode aluminum foil. The well etched Al foil can have a very uniform open-pores structure which allows a uniform dip coating of conducting polymers. The tantalum polymer capacitor starts with an oxidized sintered porous slug of tantalum powder. To create conductive polymer inside a slug with fine pores is much more difficult than creating conductive polymer on the surface of a flat aluminum foil. The polymer film inside the tantalum slug must be produced one thin layer at a time and the individual layers must communicate well with each other electrically. That is a difficult task.

#### ***b. Footprint Saving and Units Miniaturization***

Miniaturization in switch power supplies and DC/DC converters are highly desirable in space applications. Any weight loss and downsize is a plus in the design and manufacturing of space apparatus. The miniaturization is a two-fold task: reduction the number of components; and minimize the size of the components. PA capacitors with its extremely low ESR has showed significant advantage in footprint saving and component volume reduction.

This advantage can be illustrated with a ripple voltage smoothing application using PA capacitors.

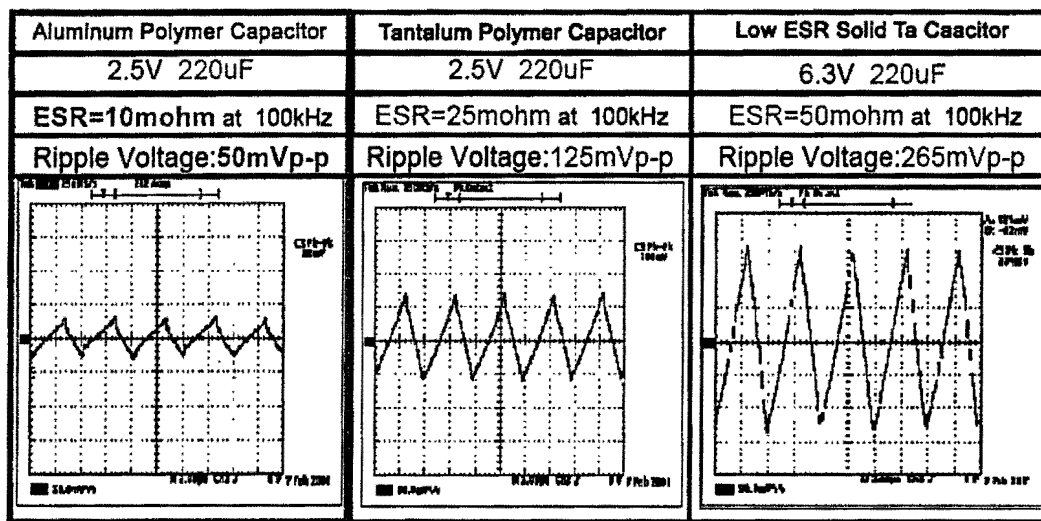


**Figure 9.** Effectiveness of Ripple Voltage Smoothing of Various Types of Capacitors (Data Courtesy of Panasonic)

When capacitors are used for IC power backup, the reduction of ripple voltage is a critical task. This task becomes more important as today's IC operation voltage becomes lower and lower. As shown in Figure 9, the reduction in ripple voltage is directly to the ESR of a capacitor. Due to its extremely low ESR, PA capacitor exhibits the best results in ripple voltage removing capability. In other words, in order to achieve the same result in ripple voltage removal, more capacitors with higher ESR are to be used together. This can be best illustrated in Figure 10.

In order to achieve comparable results in ripple removal, a single PA capacitor becomes equivalent to 3 high aqueous electrolyte aluminum capacitors and 6 fluid electrolyte aluminum capacitors. Due to the dramatic increase in ESR at low temperatures for fluid electrolyte aluminum capacitors, it will take even more conventional electrolyte aluminum capacitors to compete with PA capacitors.

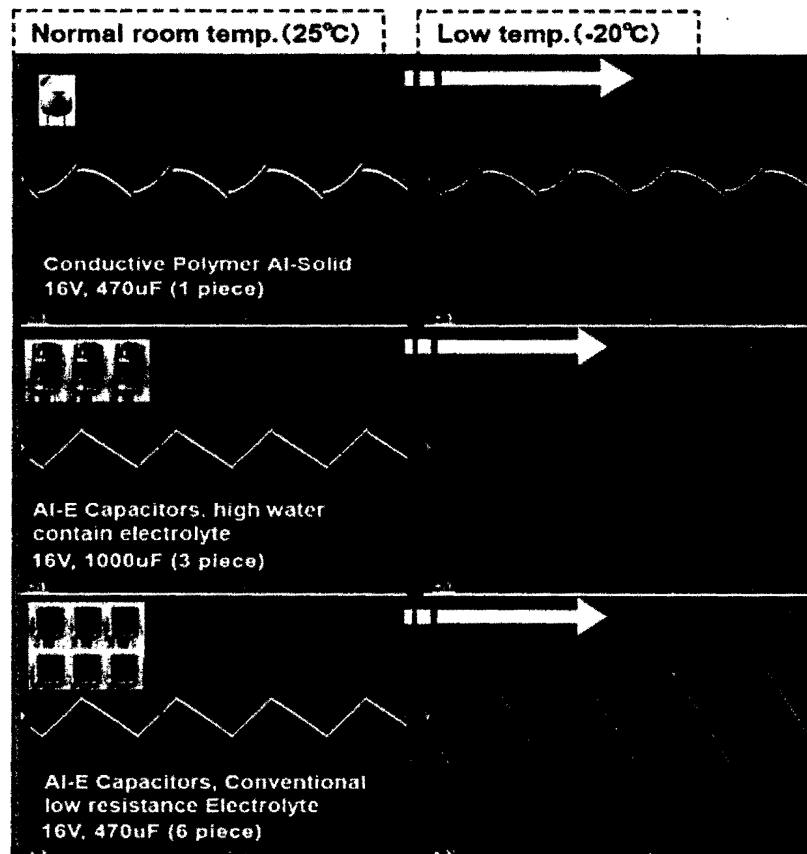


**Figure 10.** Al Polymer Capacitor equals up to six of conventional aluminum electrolyte capacitors in ripple removing application. (Data Courtesy of Japan Chemi-Con)

### *c. Benign Failure Mode*

While other capacitor types routinely fail short-circuit when exposed to over voltage or over temperature stress, both tantalum and aluminum polymer capacitors are surprisingly free of short-circuit failures. The physical mechanism that prevents short-circuit failures is in the polymer electrolyte. When a short-circuit failure tries to occur, local heating of the polymer converts it to a high resistance, stable compound, and thus effectively self heals the capacitor. On the other hand,  $\text{MnO}_2$ -based solid tantalum capacitors release oxygen that results in ignition and combustion when exposed to an overstress.

The open circuit, ignition-free failures in polymer capacitors is extremely important for space applications where the release of oxygen and combustion is catastrophic and must be circumvented.

No constituent materials are readily flammable in PA capacitors. On the other hand, even the  $\text{MnO}_2$ -free tantalum polymer capacitors will still generate substantial heat when over stressed.

A benign failure mode in PA capacitors is one of the most compelling characteristics that make PA capacitors attractive for space applications.

## Construction and Failure Modes of Polymer Aluminum Capacitors

### 1. Selection, Preparation, and Initial Electrical Characterization of Polymer Capacitors

In this study, a number of commercial available PA capacitors were selected and purchased from 5 different manufacturers. A product or a manufacturer was selected based upon the following criteria: (1). a manufacturer shall be a primary supply in polymer capacitor products. (2). the capacitor has a unique design with competitive performance. (3). priority was given to American manufacturers and their products, since it is very important to work with domestic manufacturers to develop high-rel, space grade, polymer capacitors for future NASA applications. (4). all capacitors purchased have the same footprint (EIA 7343) to facilitate the use of single PCB testing circuit.

A 20-part PCB testing card was used for the characterization of capacitors throughout this research. As shown in Figure 11, the testing card was designed with a 4-terminal to 2-terminal transition layout, which has been proven to be an accurate method for measuring capacitors.

All capacitors were solder-reflow attached on the testing card prior to testing. The soldering reflow condition follows MIL-PRF-55365G, paragraph 4.7.10. No-clean solder paste with RMA flux was used. Only one reflow cycle was applied.

All capacitors that were selected, reflowed, and tested in this research are summarized in Table I. Regular MnO<sub>2</sub> solid tantalum capacitors from manufacturer D, MnO<sub>2</sub> tantalum capacitors with a fuse design from manufacturer B, and the state-of-the-art tantalum polymer capacitors with facedown design to minimize ESL, are also included for the comparison purpose to Al polymer capacitors. The board #11 is a testing board which contains all selected capacitors. This testing board will be used for failure mode testing and will be discussed in details later.

It has been noticed that successive heat and long exposure to high temperature generated in an inappropriate solder reflow step may damage the polymer, cause early failures in MnO<sub>2</sub> tantalum capacitor, and deteriorate the capacitor's long term reliability. A proper reflow procedure will assure the good electrical contact and consistency in electrical characterizations. The capacitors after reflow were thus tested completed for capacitance, dielectric loss, ESR, and DC leakage, in order to eliminate any possible failures. The electrical testing follows the specification in MIL-PRF-55365G for tantalum capacitors, i.e., capacitance and DF at 120Hz and 1 V<sub>rms</sub>, ESR at 100 kHz, and DC leakage current at rated voltage with 5 minutes discharge time.

All measured electrical parametric data are shown in Figures 12-15. The data are presented in the format of a Weibull statistical plot with the y-axis scaled for normal probability and the x-axis for specific parameters.

As shown in Figure 12, all capacitors showed a tight distribution in capacitance. This is due to all capacitors were 100% tested at manufacturer prior to delivery. The value of slope  $\beta$  in Weibull plot here is relevant to the distribution of the parameter being tested. The higher the value of  $\beta$ , the tighter the measured parameter distribution (the parameter in Figure 12 is capacitance).

Dielectric loss (DF) data of capacitors are summarized in Figure 13. All three capacitors that are not PA capacitors exhibit the higher dielectric loss. Only the rolled foil PA capacitor from manufacturer E shows comparable DF value to these capacitors.

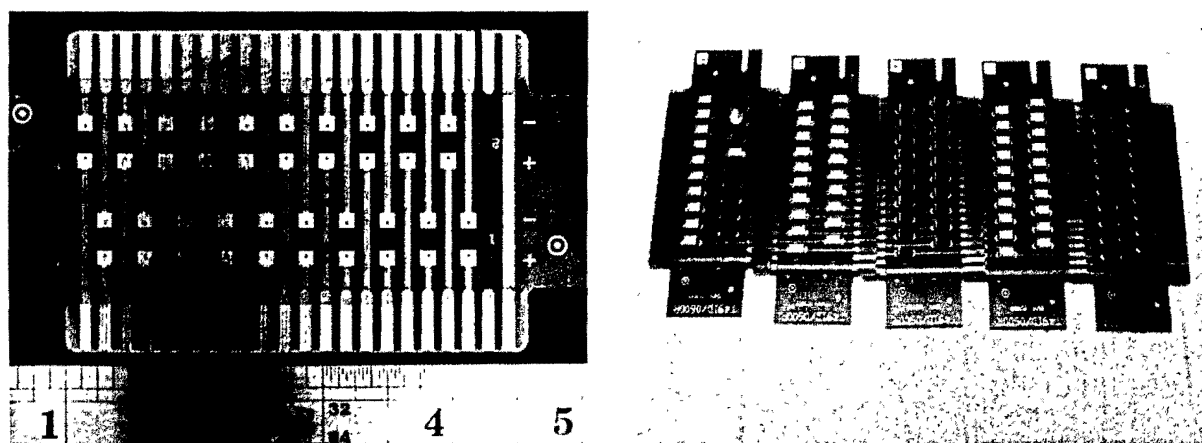
**Table I. Summary of selected capacitor samples for this research**

PCB ID	Cap ( $\mu$ F)	Rated Voltage (V)	Spec. ESR ( $m\Omega$ )	Mfg.	Cathode
Board #1	180	6.3	5	A	Al Polymer
Board #2	150	6.3	12	A	Al Polymer
Board #3	100	10.0	200	B	Solid Ta, Fused
Board #4	220	6.0	9	D	Ta Polymer, face down
Board #5	220	4.0	100	D	Solid Ta ( $MnO_2$ )
Board #6	220	6.3	15	D	Al Polymer
Board #7	100	12.0	15	D	Al Polymer
Board #8	470	6.3	8	C	Al Polymer, winding
Board #9	100	4.0	5	E	Al Polymer
Board #10	100	2.0	5	E	Al Polymer
Board #11	This board combines all the capacitors above and is used for failure modes testing (see text for details)				

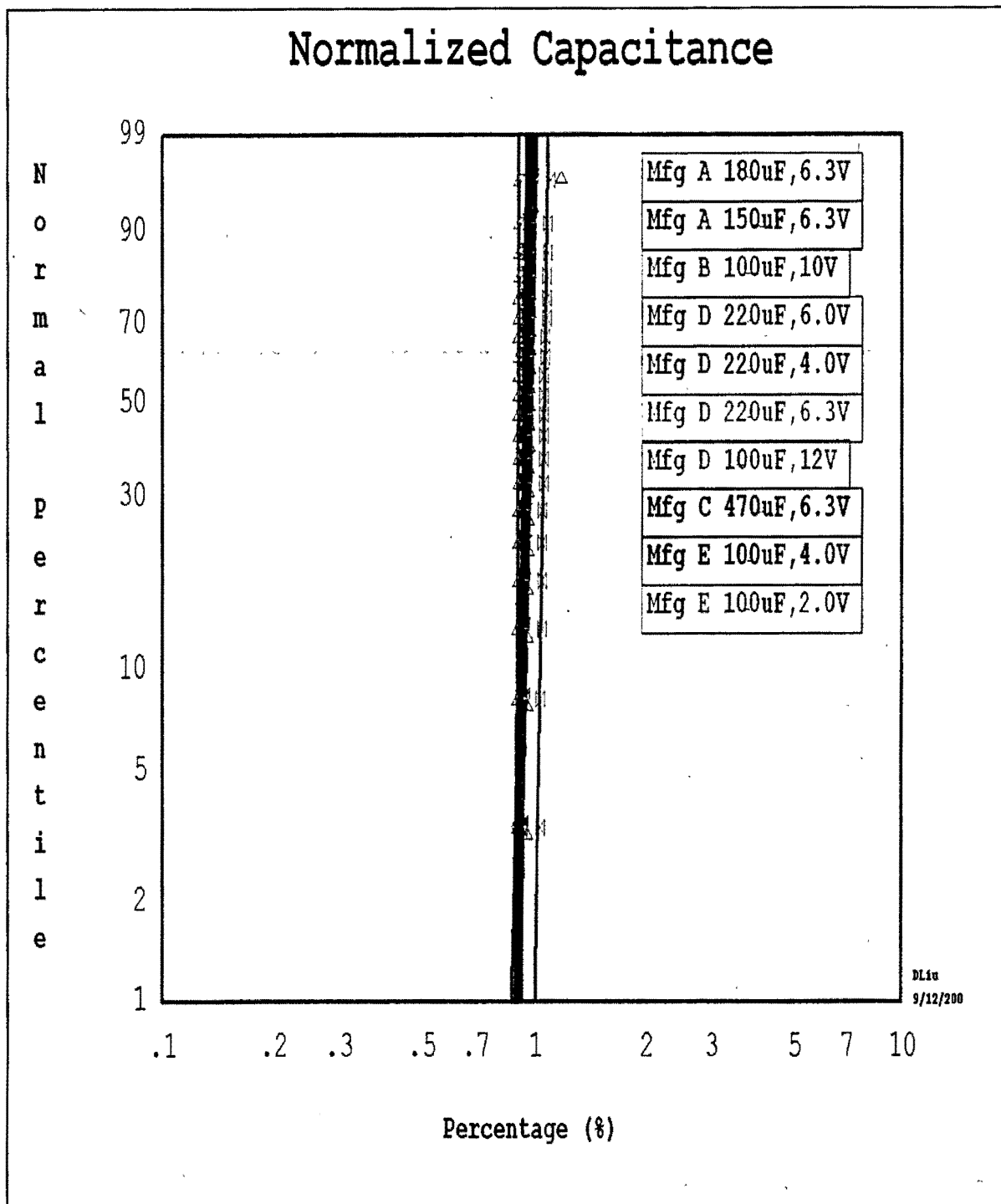
Figure 14 summarizes the 100 kHz ESR data for all the capacitors in this research. As expected, two  $MnO_2$ -based tantalum capacitors showed highest ESR values. All polymer capacitors include that of Ta polymer, with a face-down design to minimize ESL (Board #4 in Table I), showed comparable ESR testing results. In addition, most of the capacitors had ESR readings as specified in manufacturer's datasheet. ESR values as low as 3  $m\Omega$  were recorded for a 6.3V, 180  $\mu$ F capacitor made by manufacturer A (the specific ESR for this part is also marked as 5  $m\Omega$ ).

Figure 14 also shows that ESR values for various polymer capacitors are statistically uniform with nearly identical  $\beta$  value.

All capacitors were tested for DC leakage at its rated voltage with 5 minutes charge time as specified in MIL-PRF-55365G, paragraph 4.7.6. Most of PA capacitor exhibit DC leakage in the range of 0.1-1  $\mu$ A with two exceptions. The 6.3V, 470  $\mu$ F rolled foil PA capacitor made by manufacturer C showed highest DC leakage current of >200  $\mu$ A. Whether the winding construction, or the highest capacitance value among the group are the possible cause for the high leakage is not confirmed. The second worst is the Ta polymer with face-down design made by manufacturer C (Figure 15).



**Figure 11. 20-part testing card comparison before and after capacitor assembly.**



**Figure 12.** Statistic plot of normalized capacitance for all the capacitor samples listed in Table I. The capacitance was measured at 120 Hz after parts were solder reflowed to a testing card.



# Dielectrical Loss

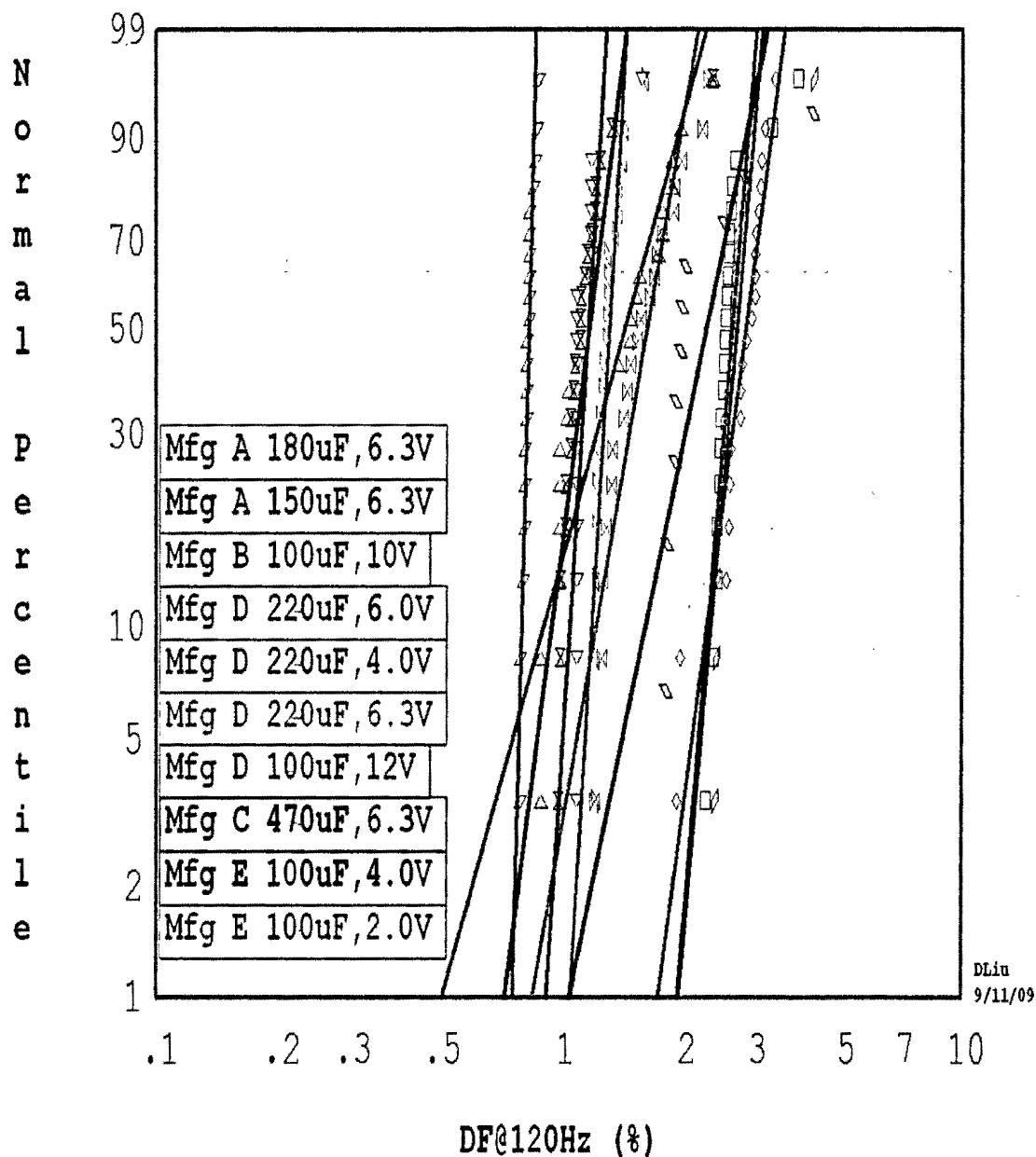


**Figure 13.** Statistic plot of dielectric loss at 120 Hz for all the capacitor samples as listed in Table I. All capacitors were measured after parts were solder reflowed to a testing card.

# Equivalent Series Resistance

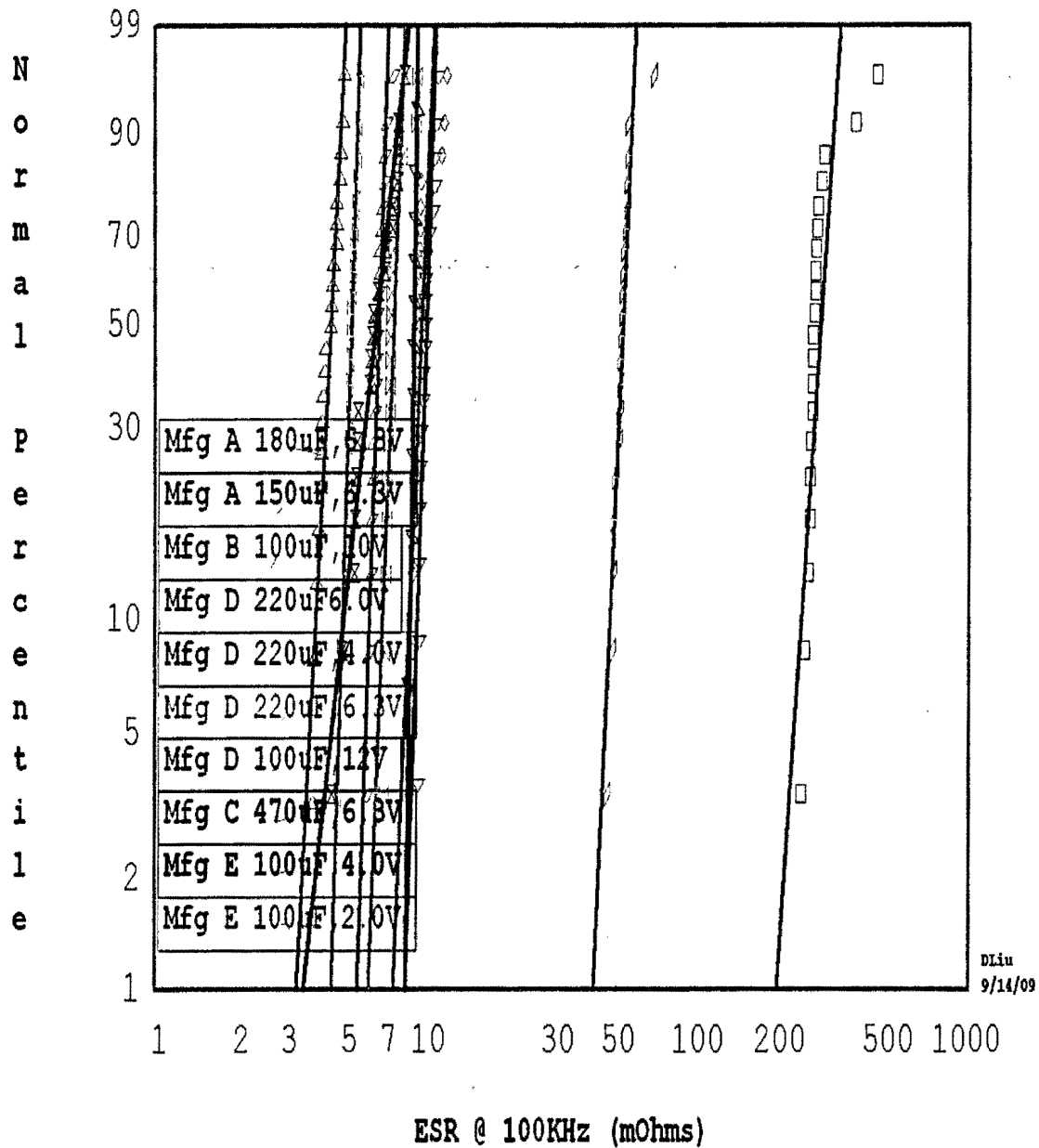


**Figure 14.** Statistic plot of ESR at 100 kHz for all the capacitor samples as listed in Table I. All capacitors were measured after parts were solder reflowed to a testing card. All PA polymer capacitors exhibit low ESR values.

## DC Leakage at Rated Voltage

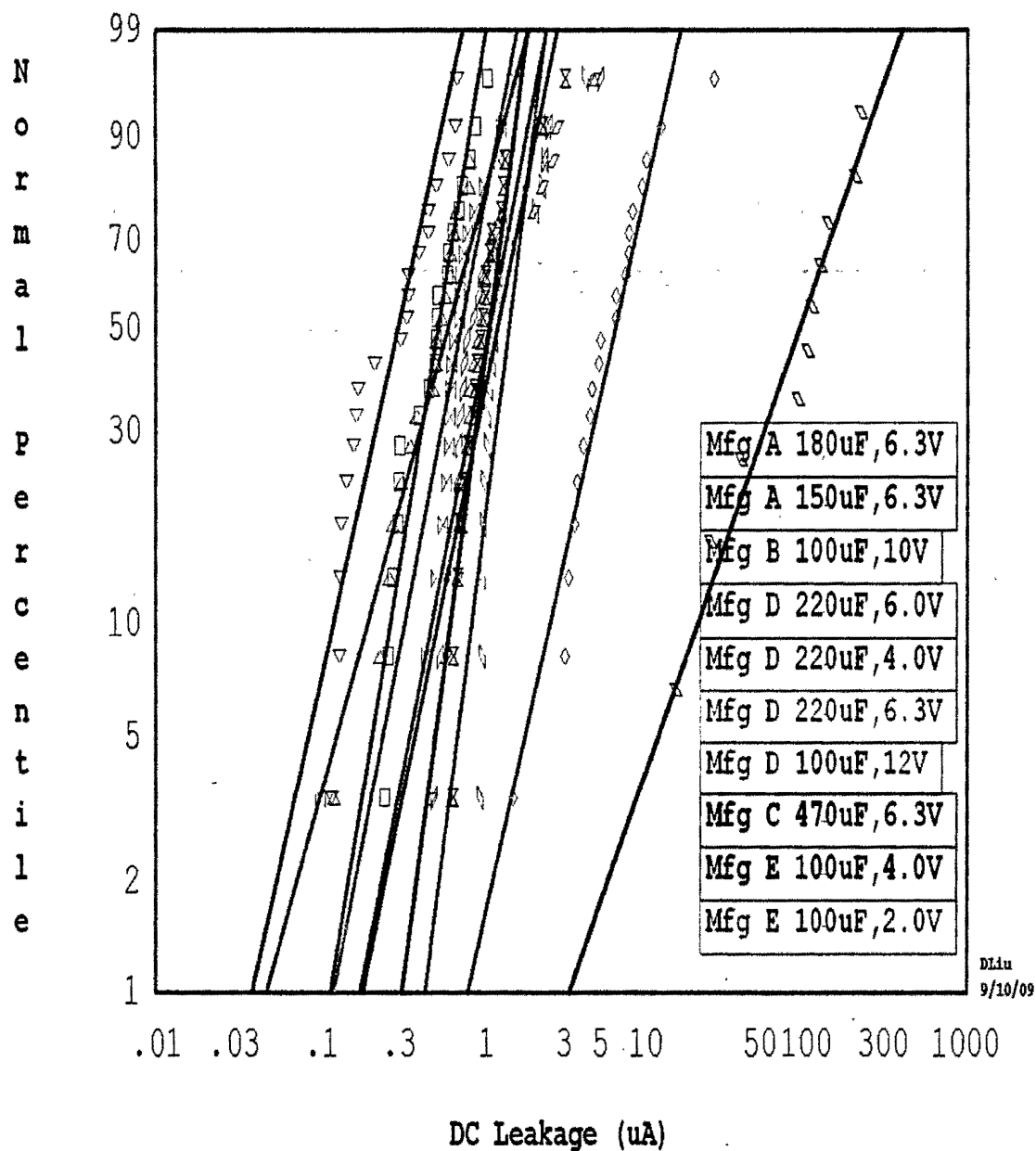


**Figure 15.** Statistic plot of DC leakage measured at rated voltage of all the capacitor samples as listed in Table I. All capacitors were measured after parts were solder reflowed to a testing card. The highest leakage capacitor is found for 470  $\mu\text{F}$ , 6.3V, with rolled foil construction made by manufacturer C. The lowest DC leakage was recorded for 6.3V, 150  $\mu\text{F}$  capacitor made by manufacturer A.

## **2. Physical Characterization of Polymer Aluminum Capacitors**

As described in the "Introduction" section, the construction of PA capacitors has been developed with different technologies (rolled foil, V-shape, etc.). Different physical styles in PA capacitor construction may impact their electrical performance. It is necessary to reveal the actual construction in details for PA capacitors.

Figure 16 combines the external and cross-section optical views as well as the top and side radiographic views of a 180  $\mu\text{F}$ , 6.3V PA capacitor made by manufacturer A. This is a commercial grade part with a total of 15 layers of etched and anodized aluminum foil stacked in a "V-shape" style. The capacitor body was encapsulated by a epoxy molding with a typical thickness of 10  $\mu\text{m}$  for the side margin and 15  $\mu\text{m}$  for the cover plate.

The cross-section electron scanning microscope (SEM) and energy dispersive X-ray (EDX) mapping images are summarized in Figure 17. This commercial part uses a 5-mil thick anodized aluminum foil with an etched tunnel having a typical depth of  $\sim 1.75$  mils at both sides of the foil. The cathode construction consisting of an over coating of carbon (graphite) followed by a silver layer bonding to the outside lead frame. The EDX mapping also reveals that the dominant elements in the conducting polymer coating are sulfur and carbon.

The 100  $\mu\text{F}$ , 10V capacitor device made by manufacturer B is a  $\text{MnO}_2$ -based solid tantalum device with a built-in fuse to prevent the short-circuit failure mode. This part was selected and used in this study for benchmarking of the performance of other PA capacitors. Therefore, the construction analysis of this part is not performed here.

The construction analysis of a 100  $\mu\text{F}$ , 10V capacitor made by manufacturer C is performed. External and cross-section optical views of the capacitor are shown in Figure 18. The results reveal that the capacitor was constructed using a so-called rolled foil technique that is conventionally used for wet electrolyte aluminum capacitors. A square plastic base was assembled at the bottom of the capacitor body, so that both anode and cathode leads can be tilted 90 degrees to achieve a surface mounting capability.

As mentioned in previous, this construction technique does not lend itself well to the applications of the polymers. In order to prevent potential rubbing of cathode foil against the anode film and creating a "short-circuit" failure, a spacer is required during the foil winding. Indeed, as shown in Figure 19, the foils were wound together so loosely that a  $\sim 2$  mil gap was created between each cathode and anode films. The existence of the gap makes the SEM and EDX examination almost impossible for this capacitor, since the foils keep drifting around when a high energy electron beam was applied to the foil material. The high-magnification optical examination reveals that anodized foil in this 10 V rated capacitor has a typical thickness of  $\sim 3.2$  mils with etched tunnel depth of  $\sim 0.8$  mils at both sides of the foil.

The optical and radiographic views of a 220  $\mu\text{F}$ , 4.0 V PA capacitor made by manufacturer D are shown in Figure 20. This commercial product exhibits a similar "V-shape" structure as that described in PA capacitor made by manufacturer A, except this capacitor only has 6 layers of stacking aluminum foils. Cross-section SEM images and 2-dimensional EDX mapping results of this capacitor are shown in Figure 21. The EDX results are very comparable to that shown in Figure 17 for the capacitor made by manufacturer A. Both capacitors use a 5-mil aluminum foil with almost the same etched tunnel depth of  $\sim 1.75$  mils, although the two devices have different rated voltages. The EDX mapping results in Figure 21 also show that the sulfur intensity is much stronger than that of carbon, while the intensities of sulfur and carbon in Figure 17 are close to each other. This indicates although the two capacitors reveal similar constructional characteristics, the conducting polymers they have used are clearly different.

Figure 22 and 23 summarize the construction analysis results for a 100  $\mu$ F, 6.0 V PA capacitor made by manufacturer E. The capacitor adapts a unique dual-layer structure that is totally different from previously described construction details. The anodized aluminum foil has a substantial big thickness of 13 mils, while the etched tunnel depth is about 5 mils on each side of the aluminum foil. The aluminum foil was only etched selectively. The non-etched end of the aluminum foil was wire-bonded directly to the lead frame for the formation of anode. The cathode, on the other hand, was formed using a nickel coated copper plate which is then sandwiched between two anodized aluminum foils.

This unique "sandwich" structure utilizes a mass of metal materials. This results in a very low ESR value (5 m $\Omega$  specified). Since only two layers of aluminum foil were used, this capacitor also has the smallest profile among all the capacitors studied in this research.

Unlike the construction of tantalum polymer capacitors which is simply a straight substitution of MnO<sub>2</sub> in the structure, the practice in polymer aluminum capacitor's construction exhibit diversified approaches. The main reason for that is the conventional rolled foil structure for wet electrolyte aluminum capacitors did not work well in the implementation of polymers. On the other hand, the existence of multiple approaches in PA capacitor construction provides opportunities for better product development. As the understanding of structure-property relationship in PA capacitors continuously makes progress, the PA capacitors can be made in such a way that a specific parameter such as ESR could be objectively enhanced.

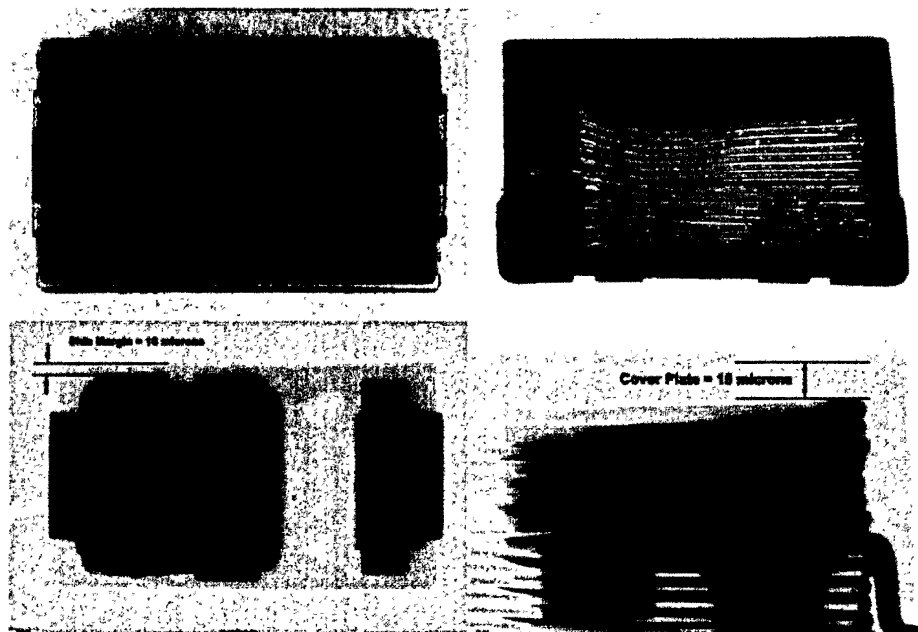


**Figure 16.** External and cross-section optical views as well as the top and side radiographic views of a 180  $\mu$ F, 6.3V PA capacitor made by manufacturer A.

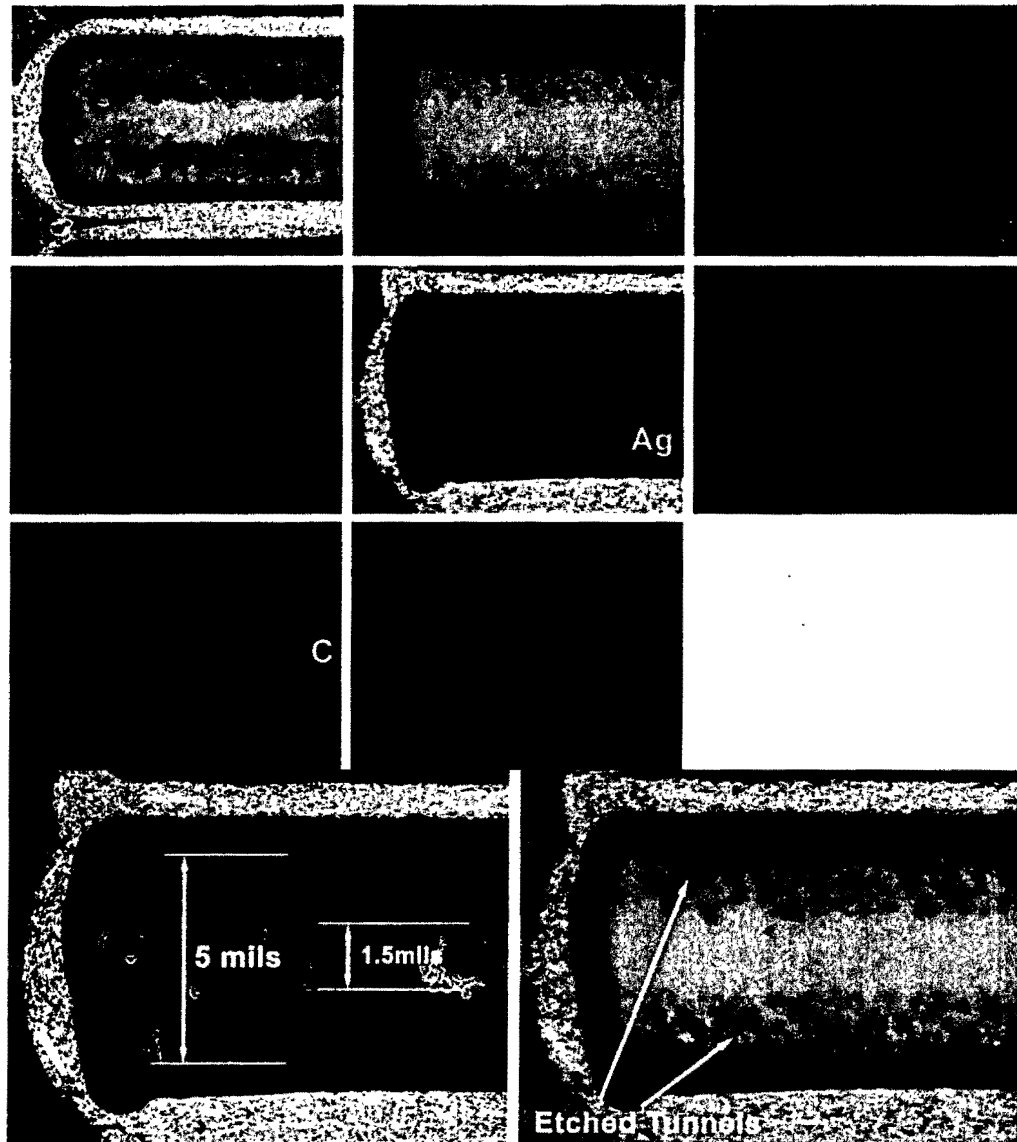


**Figure 17.** Cross-section SEM images and 2-dimensional EDX mapping results of a 180  $\mu$ F, 6.3V PA capacitor made by manufacturer A.

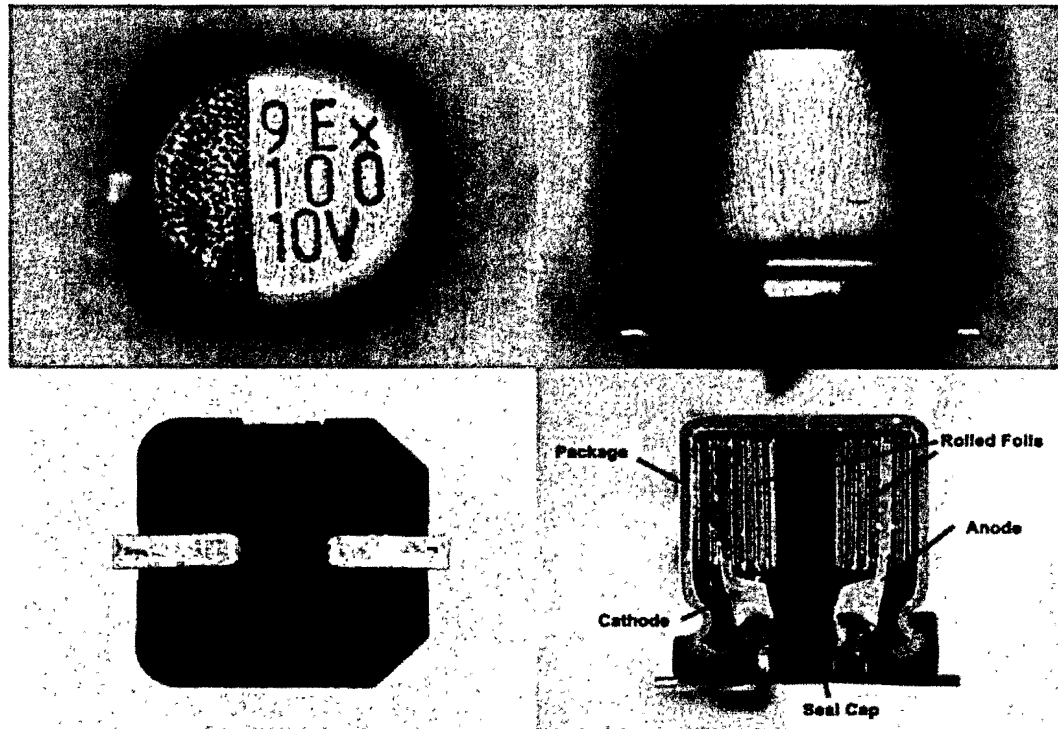


**Figure 18.** External and cross-section optical views of a 100  $\mu$ F, 10V PA capacitor made by manufacturer C. Manufacturer logo was sanitized.

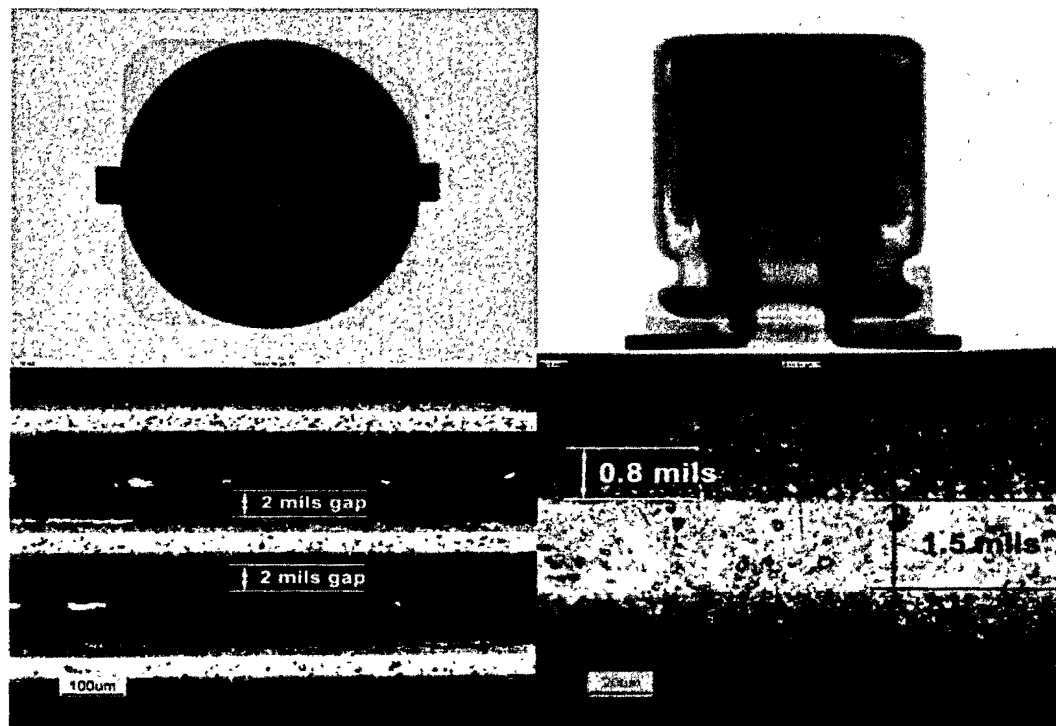


**Figure 19.** Radiographic images and high-magnification cross-sectional optical views of a 100  $\mu$ F, 10 V PA capacitor made by manufacturer C.

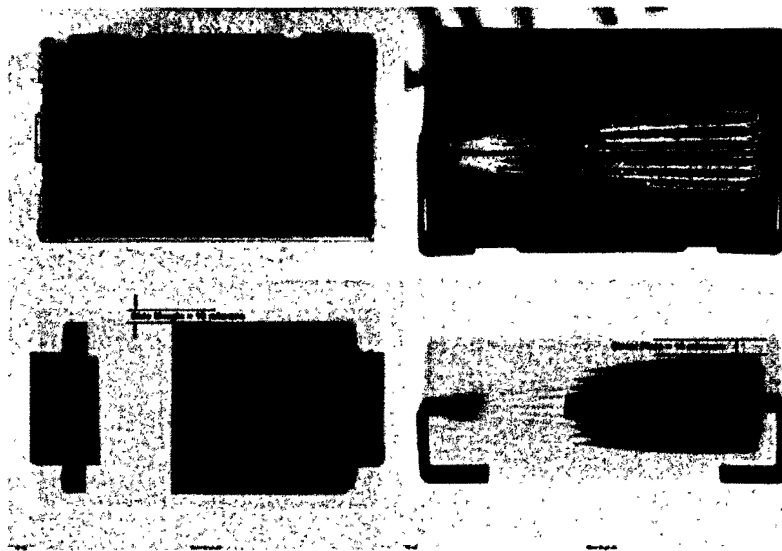


**Figure 20.** External and cross-section optical views and top and side radiographic views of a 220  $\mu\text{F}$ , 4 V PA capacitor made by manufacturer D. The device only have 6 stacking layer of aluminum foil.

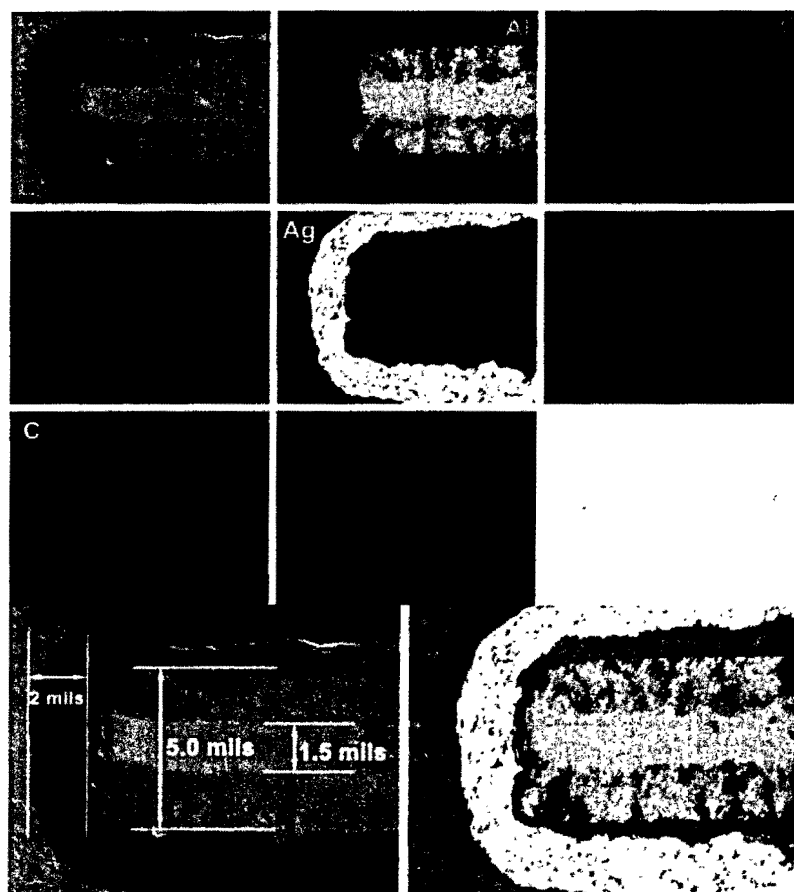


**Figure 21.** Cross-section SEM images and 2-dimentional EDX mapping results of a 220  $\mu\text{F}$ , 4.0 V PA capacitor made by manufacturer D.



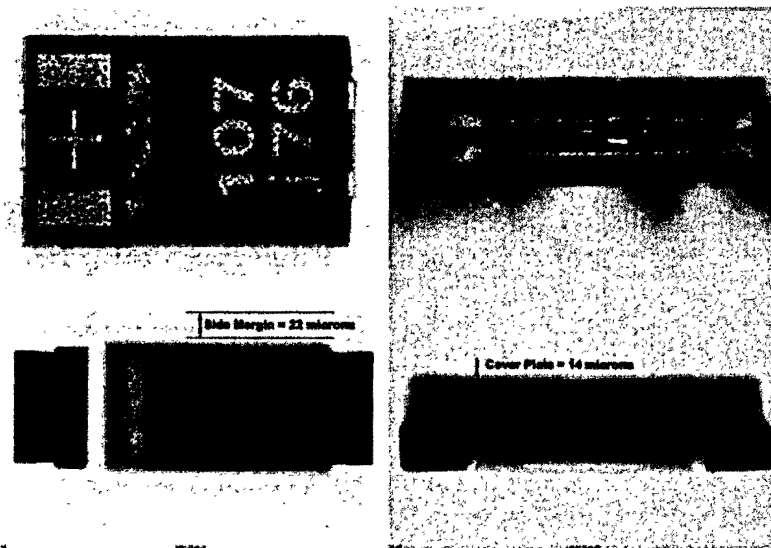


**Figure 22.** External and cross-section optical views and top and side radiographic views of a 100  $\mu$ F, 6V PA capacitor made by manufacturer E. Manufacturer logo was sanitized.

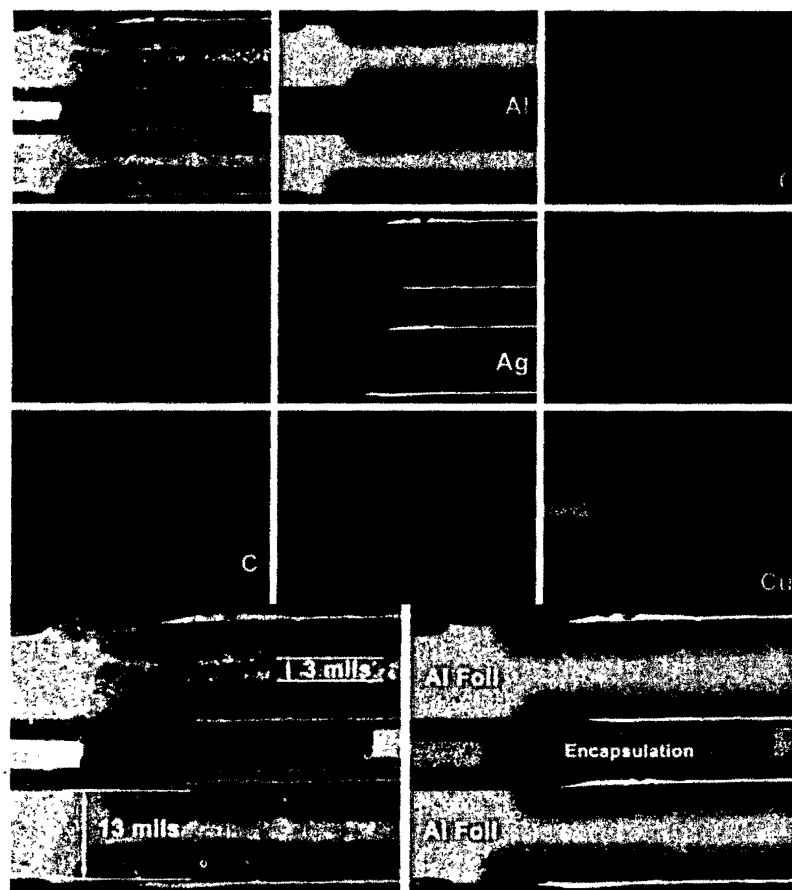


**Figure 23.** Cross-section SEM images and 2-dimensional EDX mapping results of a 100  $\mu$ F, 6 V PA capacitor made by manufacturer E.

### 3. Failure Modes in Aluminum Polymer Capacitors

One of the advantages that a PA capacitor is over a tantalum polymer capacitor is its benign failure mode which is normally open-circuit, and ignition-free. The physical mechanism that prevents short-circuit failure is in the conducting polymer electrolyte. It has been believed that when a short-circuit failure tries to occur, local heating of the polymer converts it to a high resistance, stable compound, and thus effectively self-heals the capacitor.

In order to obtain the first hand information on the failure modes in PA capacitors, a testing board was populated with different PA capacitors, some solid MnO<sub>2</sub> tantalum, and tantalum polymer capacitors. The capacitors were electrically tested for capacitance, DF, ESR, and DC leakage prior to board assembly.

All capacitors on the board were pushed to failure by applying a reverse voltage that was twice the rated voltage of the capacitor. A power supply capable of delivering 20 amps continuous current is used to provide massive reverse current to the capacitor. With such a set up, a capacitor can be killed very quickly due to a massive current flow. Figure 24 compares the same testing board before and after the "pushing to fail" test. Various polymer capacitors were placed alternatively with MnO<sub>2</sub> tantalum capacitors. All MnO<sub>2</sub> parts were assembled on the odd numbered locations (top row in Figure 24), and failed in sustained combustion (some failure procedure were video recorded for documentation). On the other hand, all the PA polymer parts failed without ignition and most of them did not even show mild scorching.

The push to fail testing results showed two exceptions. A 220  $\mu$ F, 6.0V PA capacitor made by manufacturer D showed case cracking during the test although there was no evidence of any ignition or "smoke" (Figure 25 (A)). Another 220  $\mu$ F, 6.3V tantalum polymer capacitor made by manufacturer D showed discoloration in the middle area of epoxy mold and a part displacement from the solder pads (Figure 25 (B)). This may be explained that when the part was reversed biased at 2X rated voltage and with sustained continuous I<sup>2</sup>R heating the substantial heat generated might have caused combustion of the plastic case and the melting of the eutectic solder. Table II summarizes the details on the failure information for all capacitors on the testing card.

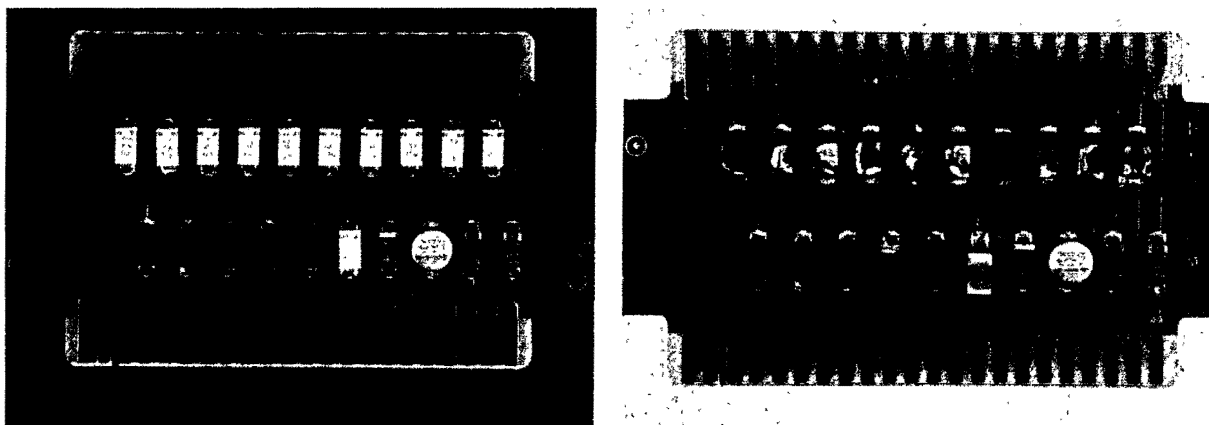
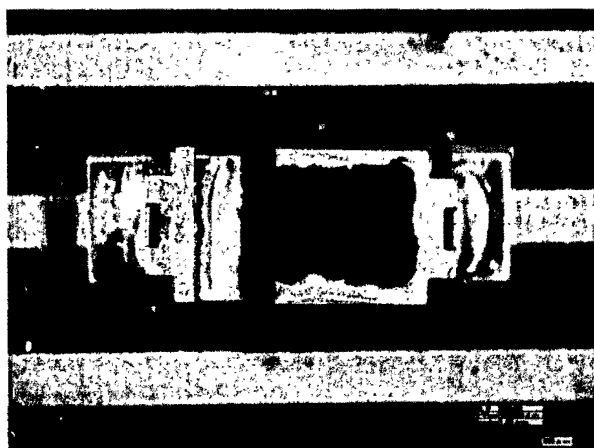
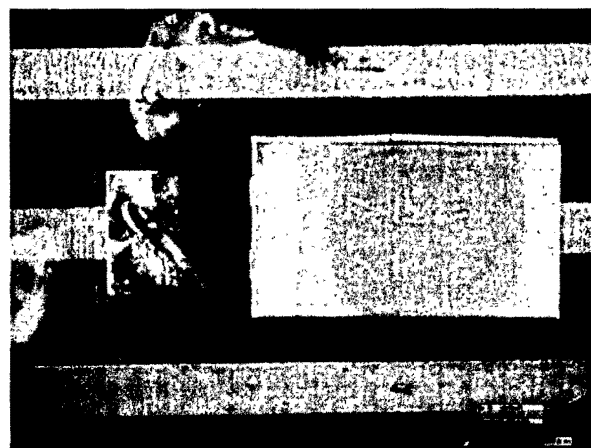


**Figure 24.** Comparison of testing board#11 before and after "push to fail" testing which killed the capacitors with massive current flow at twice the rated voltage in a reversed bias condition. All MnO<sub>2</sub>-based tantalum capacitors (top row) failed and ignited, whereas most of polymer aluminum capacitors showed no evidence of ignition.



(A)



(B)

**Figure 25.** Optical views of two polymer capacitors which revealed some damages after push to fail test. (A). A PA capacitor showed case cracking; (B). Discoloration and a part displacement were observed in this tantalum polymer capacitor with a face-down design to minimize the part ESL.

Table II. Failure Descriptions of All Capacitors on the Testing Board#11

Number of location on Board	Manufacturer	Cap (μF)	Rated Voltage (V)	Cathode	Failure description
All odd numbers	D	220	6.0	MnO <sub>2</sub> Ta	All failed in sustained combustion, resistance reading between R= 5-1500 Ω after failure
2	A	180	6.3	Al Poly	R=1.7 Ω, no visible damage
4	A	150	6.3	Al Poly	R=22 kΩ, no visible damage
6	D	22	16.0	Al Poly	R=3.3Ω, no visible damage
8	D	220	6.3	Al Poly	R=1.2 kΩ, case cracking (Fig. 21 A)
10	D	100	12.0	Al Poly	R=2.1 Ω, no visible damage
12	D	220	6.3	Ta Poly, face down	R=open, part displacement, package discoloration (Fig.21B)
14	B	100	10.0	MnO <sub>2</sub> Ta, fused	R=open, no visible damage
16	C	470	6.3	Al Poly	R=15.8 kΩ, no visible damage
18	E	100	4.0	Al Poly	R=1.5 Ω, no visible damage
20	E	100	2.0	Al Poly	R=1.1 Ω, no visible damage

## Electrical Characterization in Frequency and Temperature Domain

Capacitance and ESR data versus frequency and temperature are presented in this section for all the PA capacitors and other benchmarking tantalum capacitors. As per MIL-PRF-55365, only 120Hz capacitance and 100 kHz ESR are to be specified for a tantalum capacitor, however, a tantalum capacitor is seldom used in circuits operating at 120 Hz. Most of power supplies and DC/DC converters in nowadays cover a frequency range from kilohertz to Megahertz. In addition, few circuits operate at 25°C. More typically, capacitors have to be operated in a temperature range from below room temperature to as high as 125°C. As a possible substitution to MnO<sub>2</sub>-based tantalum capacitors, PA capacitors need to be electrically characterized in both frequency and temperature domains.

The frequency domain dielectric response of a capacitor highly depends on its construction technology. Most of PA capacitors are created with the formation of fine etched tunnels on both sides of an aluminum foil. This porous tunnel structure provides a substantial surface area for the dielectric layer constructions with high capacitance. It will take time for external electrical signal to conduct to the very inner parts of a fine tunnel structure through conductive polymer electrolyte.

At low frequencies (longer time), there is enough time for capacitance inside the tunnel to be fully charged to the externally applied voltage, which means all the inner tunnels can be “seen” by the external circuit. At high frequencies, the rate of charging inside the tunnel is limited by RC constants along the electrolyte’s path and the tunnel’s internal capacitance is no longer “keeping up” with the time-varying changes of external voltage. As external signal frequency goes higher, more and more tunnels are not able to “see” the external circuit anymore. As a result, there exists a characteristic frequency  $f_c$  beyond which the effective capacitance of the structure begins to predictably decline. This behavior is observed for all capacitors and is known as “capacitance roll-off”. A capacitor with a so-called better high-frequency performance typically means it possesses a higher value of  $f_c$  and with less capacitance drop beyond the  $f_c$  (Figure 7).

In this research, the PA capacitors are characterized using an Agilent 4294A Precision Impedance Analyzer in the frequency range from 100Hz to 10MHz. The RF testing fixtures are 4-terminal, 1-meter cable assemblies of which the high-frequency performance is optimized. The capacitor samples are electrically selected prior to being soldered at the ends of the RF cable assembly. The frequency domain testing set up is shown as Figure 26.

The temperature range of frequency-domain characterization for PA capacitors was extended on the cold side beyond the normal military temperature range of -55°C to 125°C. In a previous NEPP fund program, the tantalum polymer capacitors were characterized at a temperature as low as -194°C (boiling point of liquid nitrogen). In order to compare the PA capacitor with tantalum apple-to-apple, the effort was also made to test PA capacitors at such low temperatures. However, due to a delay in the construction of liquid nitrogen drop lines in the laboratory, the low temperature testing could only be performed at -95°C for FY09. The RF characterization of PA capacitors at lower temperatures should be continued in FY10.

Capacitance and ESR versus frequency data for two PA capacitors are shown in Figure 27. Both capacitors are 6.3 V rated, with an EIA 7343 footprint, and made by manufacturer A. Only difference is in the specific capacitance and ESR: 180  $\mu$ F versus 150  $\mu$ F, 5 m $\Omega$  versus 12 m $\Omega$ . The left-hand graphs are capacitance versus frequency and the right-hand graphs are ESR versus frequency. This format allows direct comparison of the relative performance of the competing technology and manufacturers and will be used for the rest of this section.

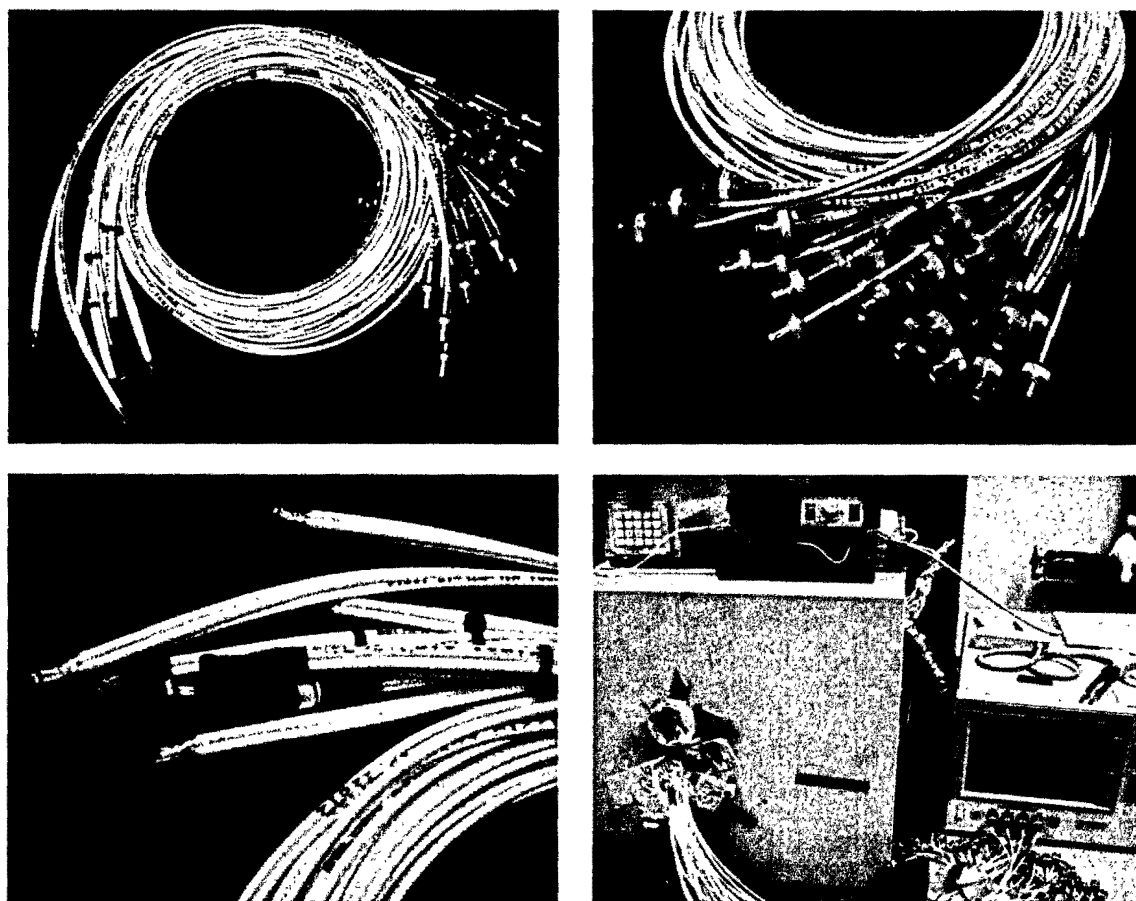


**Figure 26.** RF cable assembly and the testing set up for the characterization of PA capacitors at a range of temperatures.

As shown in Figure 27, both PA capacitors exhibit a constant response with frequency and slight dependence on temperature change. No capacitance roll-off is observed up to 200 kHz. ESR versus frequency curves show a “bath tab” shape with ESR falling at lower frequencies, leveling off at the middle frequencies, and rising slightly and higher frequencies. This ESR versus frequency change can be explained briefly as following: Total ESR comprises contributions from both dielectric loss of the oxide film which falls rapidly with increasing frequency and contact resistance in the electrolyte layers of either  $\text{MnO}_2$  or conducting polymer which are typically constant with frequency. As frequency goes around 1MHz, skin effect becomes dominant which result in resistance increase with frequency.

Figure 28 compares capacitance and ESR versus frequency for three different capacitors. The two plots at top present frequency responses of the  $\text{MnO}_2$ -based tantalum capacitor of 220  $\mu\text{F}$ , 10V and with a built-in fuse made by manufacturer B. The roll-off of capacitance is clearly evident for this part beginning at 10 kHz. Moreover, as ambient temperatures falls, the roll-off frequency shifts to ever-lower frequencies. When temperature is below  $-15^\circ\text{C}$ , more than 50% of capacitance at 100 kHz is gone.

On the other hand, two polymer capacitors shown in Figure 28 show very little capacitance roll-off after 100 kHz. Bearing in mind that 470  $\mu\text{F}$ , 6.3 V, 8 m $\Omega$  ESR capacitor made by manufacturer C is the only one that with a rolled foil construction. The lower frequency appearance of capacitance roll-off (100 kHz) may have been contributed to the loose structure of the capacitor with extraordinary high dielectric loss and DC leakage (Figs. 13 and 15).

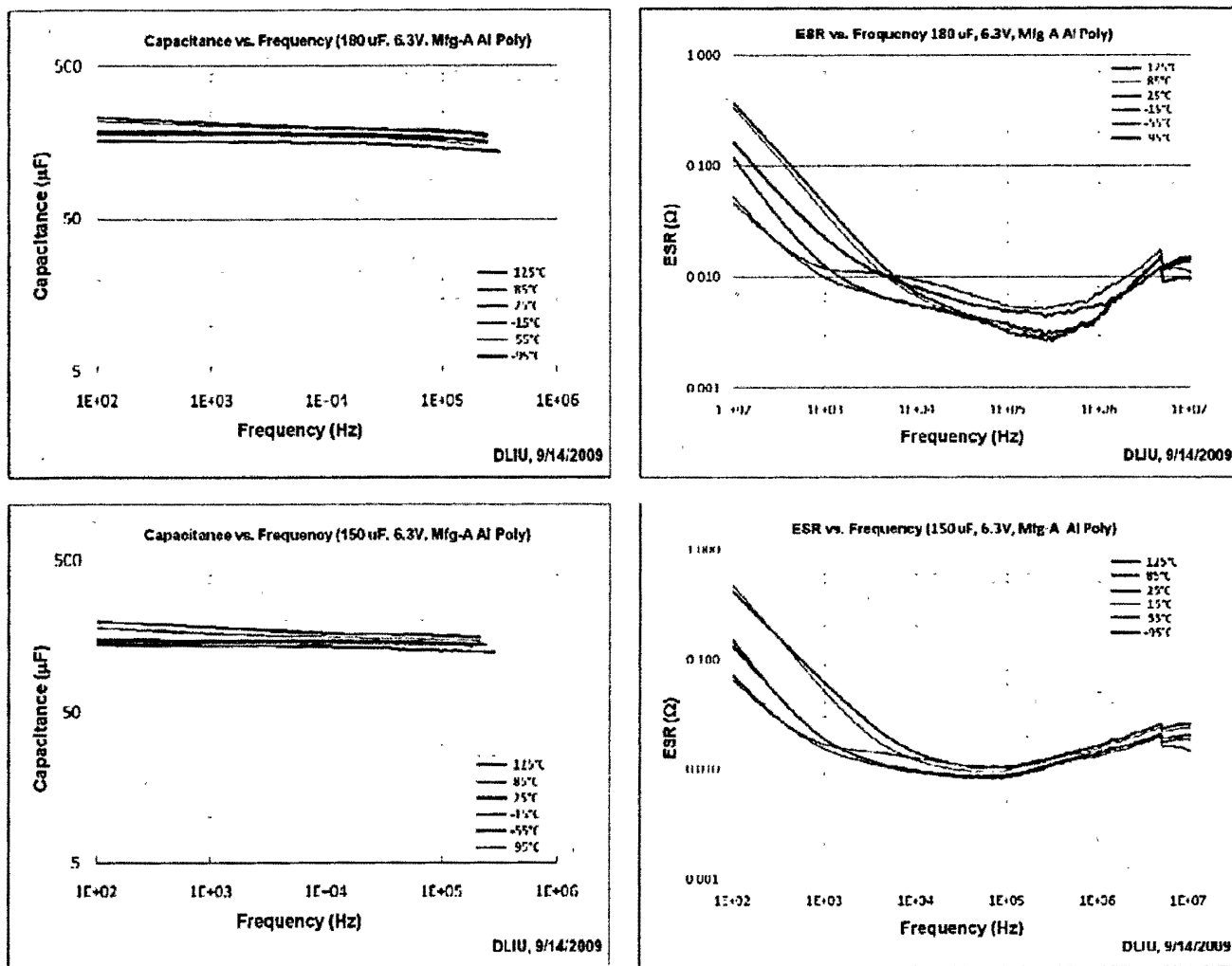


**Figure 27. Capacitance and ESR vs. Frequency at Various Temperatures for 6.3V, 180 µF and 150 µF Aluminum Polymer Capacitors Made by Manufacturer A.**

The two bottom plots present the frequency performance of a tantalum polymer capacitor with a face down design to facilitate low ESL. Note the actual measured ESR for this part is about 10 mΩ at 100 kHz (specified ESR is 9 mΩ), which is relatively high in comparison to ESR values of most aluminum polymer capacitors investigated in this research.

The capacitance and ESR versus frequency data of three capacitors all made by manufacturer D are present in Figure 29. The two top plots show the frequency performance of a MnO<sub>2</sub>-based tantalum capacitor. As expected, the capacitance roll-off occurs at ~10 kHz at 125°C and the  $f_c$  decreases dramatically with decreasing temperature. The  $f_c$  is about 2 kHz at -95°C. The poor low-temperature performance is a significant limitation of MnO<sub>2</sub>-based technique. On the other hand, the capacitance roll-off is very minor and is almost not affected by decreasing temperatures. This is a significant advantage of polymer aluminum capacitors.

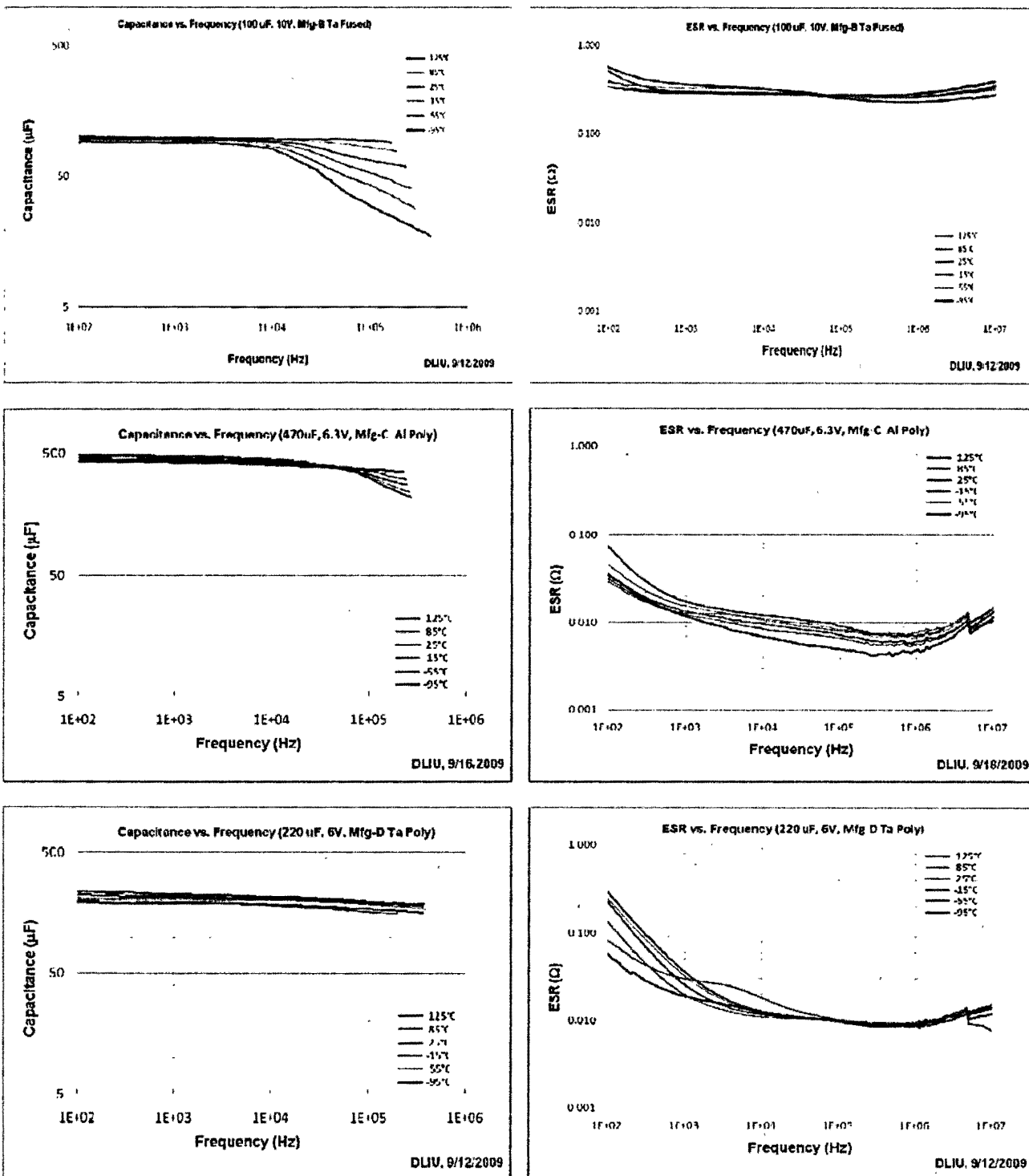


**Figure 28.** Capacitance and ESR vs. frequency at various temperatures for 10V, 100  $\mu$ F fused  $\text{MnO}_2$ -tantalum capacitor made by manufacturer B (top), for 6.3V, 470  $\mu$ F Al polymer capacitor made by manufacturer C (middle), and for 6.0V, 220  $\mu$ F Ta polymer capacitors made by manufacturer D (this capacitor has a measured ESR of 9 m $\Omega$  at 100 kHz as specified (bottom)).

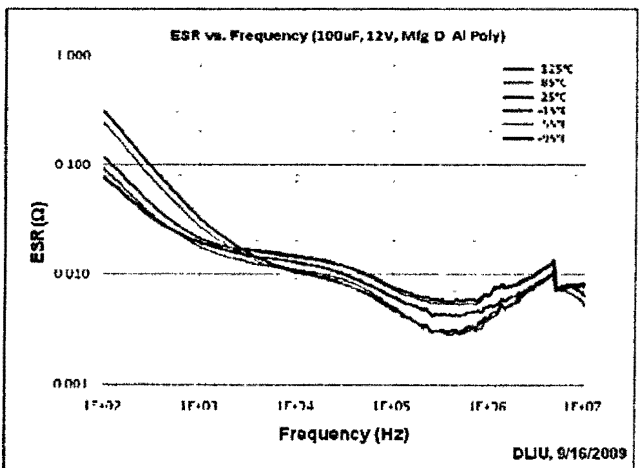
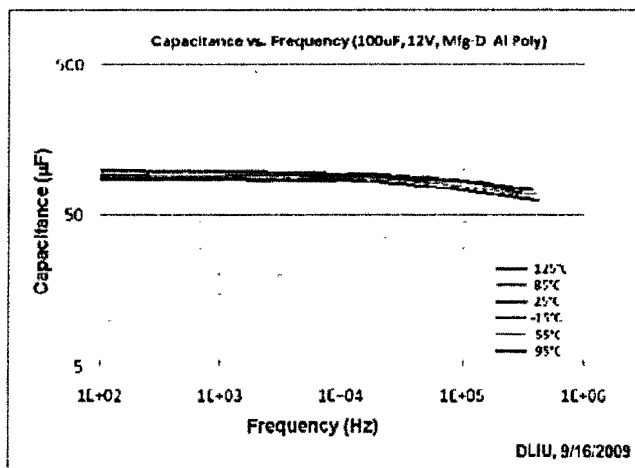
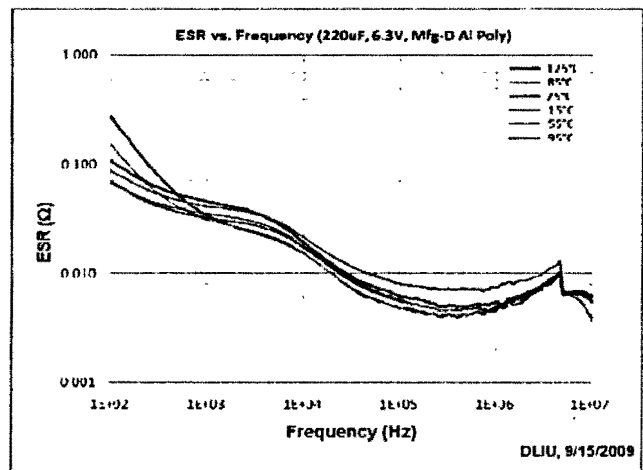
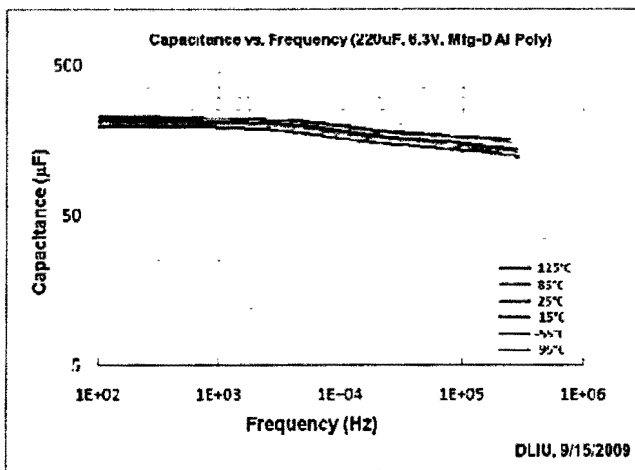
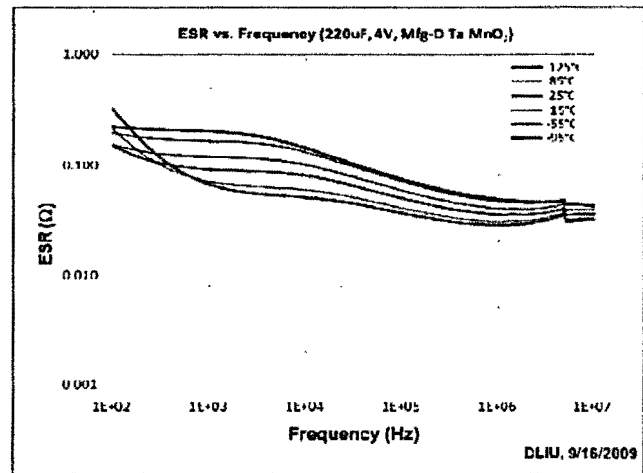
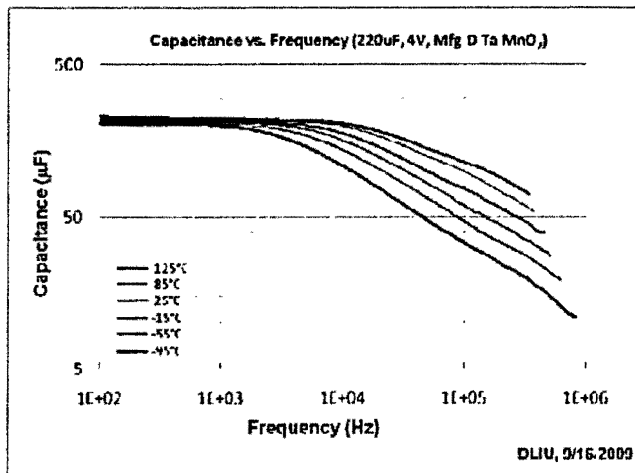


**Figure 29.** Capacitance and ESR vs. Frequency at Various Temperatures for 4V, 220 μF MnO<sub>2</sub>- Tantalum Capacitor (top), for 6.3V, 220 μF Al Polymer capacitor (middle), and for 12V, 100 μF Al Polymer Capacitors (bottom) All Made by Manufacturer D. Please Note the ESR of MnO<sub>2</sub>-Based is about 10 Times Higher Than Those of Al Polymer Capacitors.



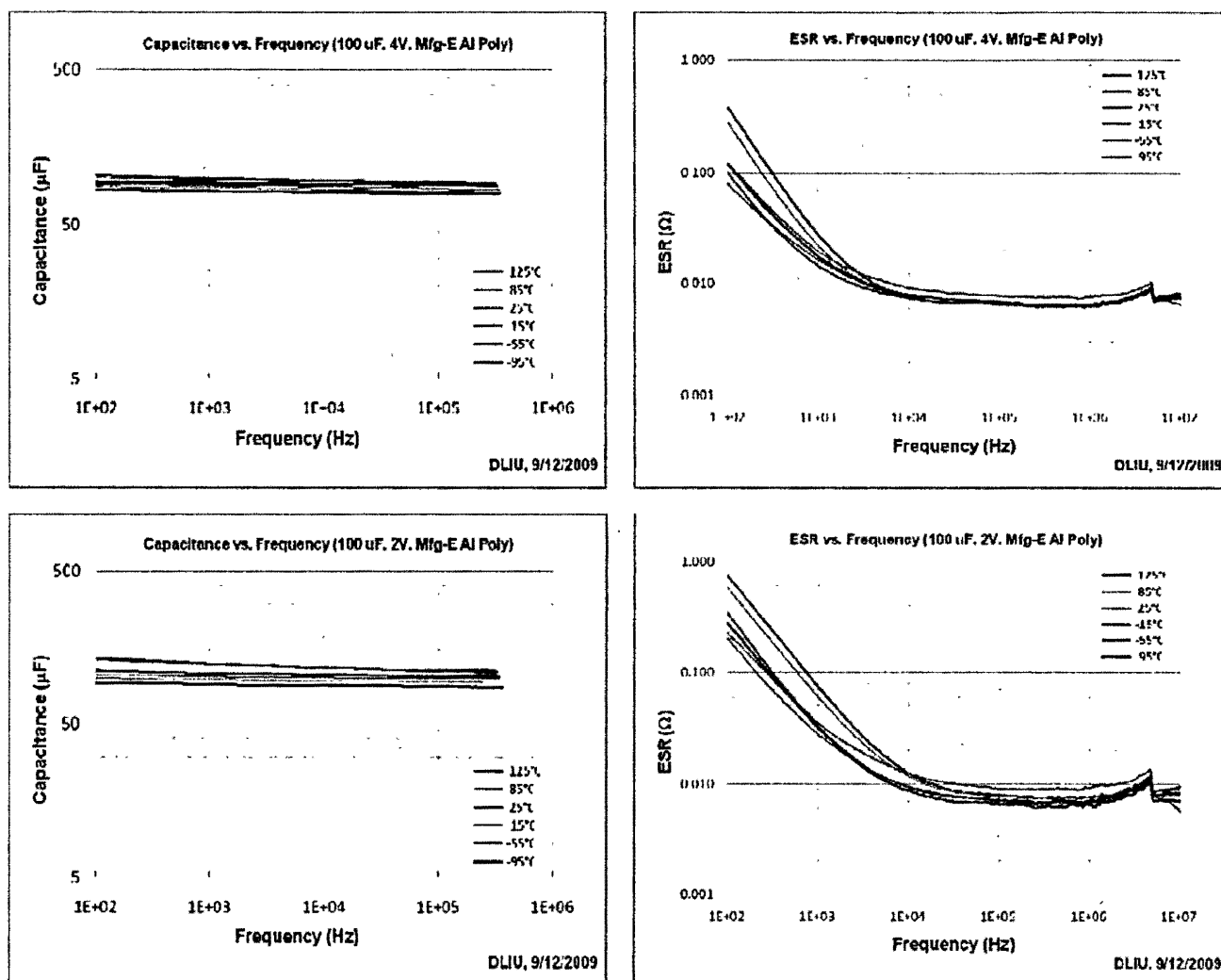


**Figure 30.** Capacitance and ESR vs. Frequency at Various Temperatures for 4V and 2V, 100  $\mu$ F Al Capacitor made by Manufacturer E (top). Note the Measured Capacitance Shows Almost Independent to Temperature and frequency.

The best performance data of capacitance versus frequency are revealed for two PA capacitors with low rated voltage made by manufacturer E. As shown in Figure 30, the capacitance data at various temperatures exhibit almost straight lines versus frequency and do not change much with temperature. The capacitance at 100 kHz only decreased from 93.4  $\mu$ F at +125°C to 80.8  $\mu$ F at -95°C, a 13.5% decrease with a broad temperature range of more than 200°C! The measured values of ESR of 6.4 m $\Omega$  for the two capacitors are slightly higher than the specified value of 5 m $\Omega$ , but not in significantly difference. So far, no any other capacitor technology can achieve a comparable frequency performance and low ESR as present here for this 4V, 100  $\mu$ F, and 5 m $\Omega$  ESR polymer aluminum capacitor made by manufacturer E.

As previously discussed in the capacitor construction section, these low voltage PA capacitors revealed a unique “sandwich” structure which is different to both the V-shape construction and the conventional rolled foil approach. Whether or not this unique capacitor structure has anything to do with its extraordinary performance, it needs to be further investigated.

## Thermal Vacuum Testing of Aluminum Polymer Capacitors

Thermal vacuum testing is a thermal cycling test that is performed at low pressures ( $10^{-4}$  Torr typical). In general, the thermal vacuum test imposes an environment that simulates orbital conditions more accurately than any other ground test. A thermal vacuum test help screening for the defects that are detectable by a thermal cycle test as well as the defects that would respond only to a vacuum environment. Such vacuum-related phenomena as arcing and multipacting/corona, plus certain materials outgassing problems, can be found only under thermal vacuum conditions.

Arcing is an energy transfer process from DC powered source whose likelihood increases at low pressures, high voltage ( $>150\text{V}$ ) and short distance between electrodes. Multipacting/corona is an electron transfer process at low pressures. The pressure is so low that the mean free path of electrons is longer than the electrode separation distance. Thus, the electrons can readily travel between the electrodes without undergoing collisions with the gas molecules. In comparison to arcing, Multipacting/corona is an energy transfer process from AC-powered source whose likelihood increases as in arcing but also with increased frequencies. Multipacting breakdown voltage is usually lower than that of arcing. Out gassing is an ejection of gases or water vapor that has been trapped in a material. The unique thermal vacuum environment promotes the phenomenon.

According to MIL-STD-1540, all high-orbit systems and vehicles are required to undergo thermal vacuum testing. MIL-HDBK-340 and NASA standard GSFC-STD-7000 define the test level and duration not only for systems and vehicles, but also extended to subsystem and unit levels.

Although the component/part level thermal vacuum test is not required, it is still valuable to examine the thermal vacuum performance of polymer aluminum capacitors. The multipacting breakdown has been thoroughly studied in RF coaxial transmission cable assemblies. It concludes that multipacting breakdown voltage is a function of operation frequency and the electrode distance (voltage versus MHz-cm).

A number of studies have shown that the worst frequencies for multipacting breakdown are between 500 MHz and 2.5 GHz. At low voltage levels (less than 20 V) and low average power (less than 8 W), multipacting breakdown is theoretically impossible. Since most of PA capacitors are used in several hundreds kilohertz and its power level is much less than 8 watts, the potential risk of multipacting breakdown for PA capacitors could be neglected. In addition, when populated on the PCB circuits for spacecraft applications, the board is either epoxy potted or thermal paralene coated which further reduces the risk of multipacting.

Accordingly, the thermal vacuum testing in this research will be mainly focused on possible outgassing problems. Based on the guidelines in MIL-HDBK-340A, Vol. 1 and GSFC-STD-7000, a thermal vacuum cycling profile was determined as following:

Pressure:  $10^{-5}$  Torr  
Temperature: Hot limit =  $+105^{\circ}\text{C}$ ; Cold Limit =  $-44^{\circ}\text{C}$ .  
Duration: 12 Cycles.

All capacitors are visually inspected and electrically tested for capacitance, DF, ESR, and DC leakage as per MIL-PRF-55365G, before and after thermal vacuum testing. Figure 31 shows the actual thermal vacuum cycling profile. All the testing data are presented in a statistic plot format as shown in Figure 32. The capacitance and DC leakage are not evidently changed before and after test, whereas DF and ESR show slight decrease after testing. The decrease in DF and ESR after thermal vacuum testing might have been due to the fact that thermal vacuum test promoted the escaping of trapped water vapors from the epoxy molding. Visual inspection after the test did not show any detectable damages.

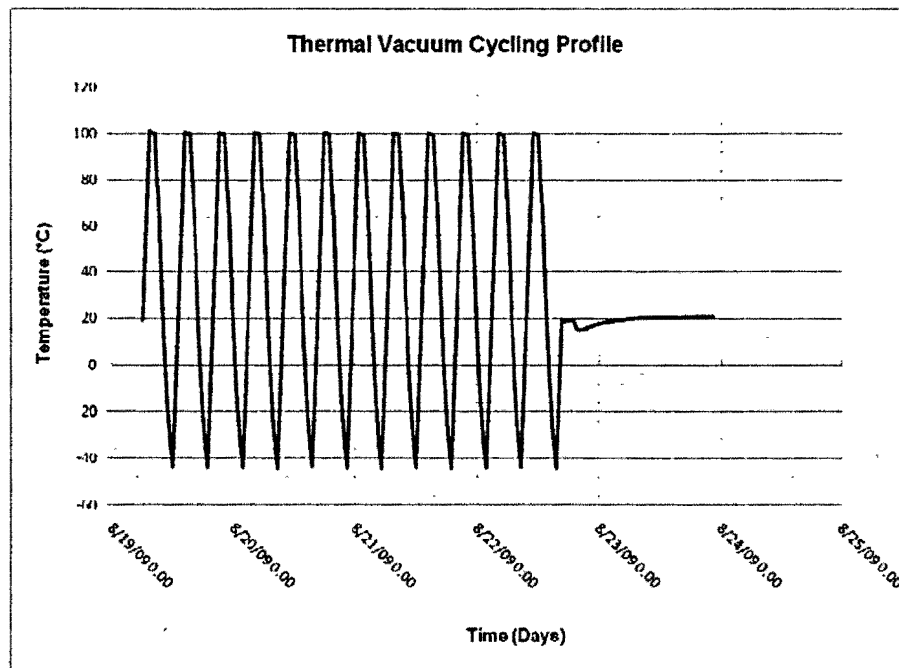


Figure 31. Actual thermal vacuum cycling profile for testing of PA capacitors.

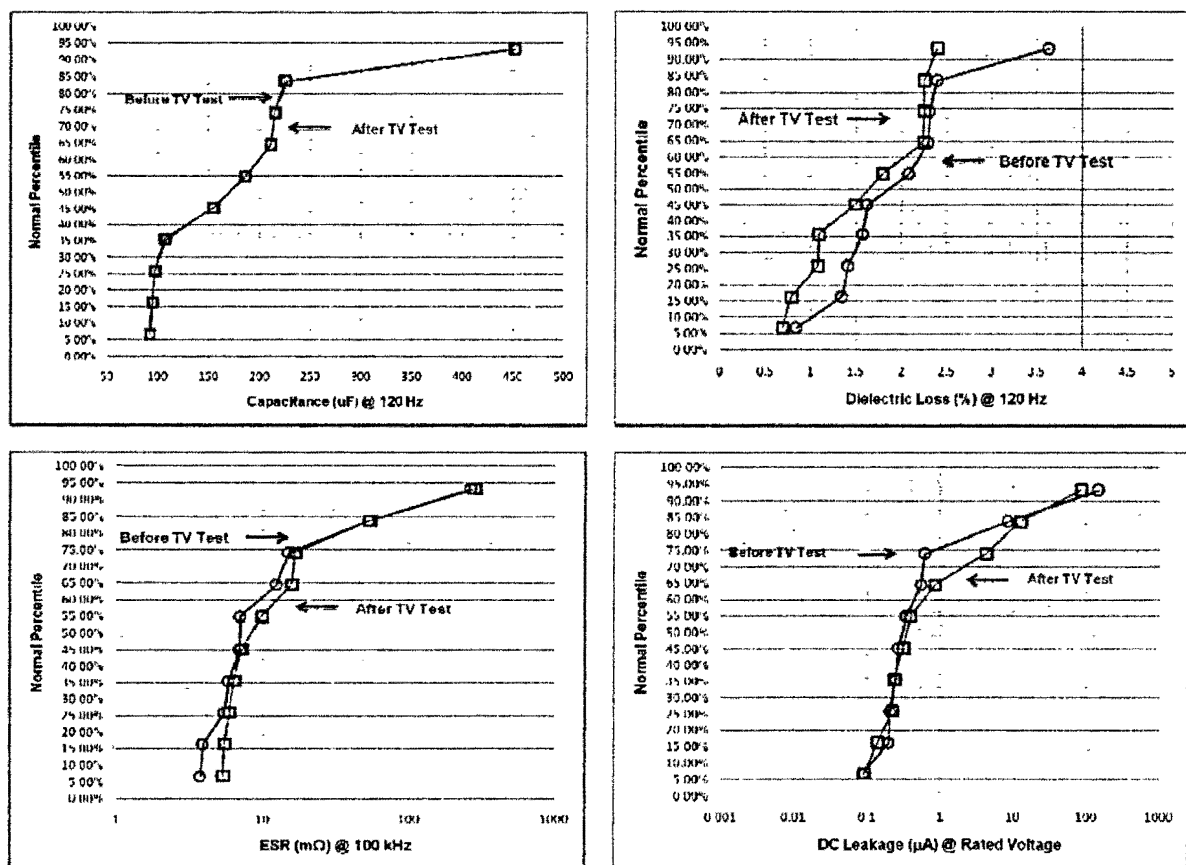


Figure 32. Statistical plots of capacitance, DF, ESR, and DC leakage of capacitors before and after thermal vacuum testing.

## Steady Step Surge Testing of Aluminum Polymer Capacitors

A prevalent failure for MnO<sub>2</sub>-based tantalum capacitors is the power-on failures. The capacitor can be electrically broken down even below the rated voltage due to rapidly changed, high current turn-on pulses (a surge current). A test is designed and applied to screen out these early failures has been widely applied to tantalum capacitors. This test is called steady step surge test (SSST test).

This test consists of rapidly charging the capacitors with incremented voltage through low series resistance. All capacitors under test were solder-reflow assembled to a PCB test card prior to SSST test. When test begins, the capacitor is charged to a set voltage, held at that voltage for ½ second, and then discharged through a low resistor ( $<0.5 \Omega$ ) for ½ second. This sequence is repeated five times (as shown in Figure 33).

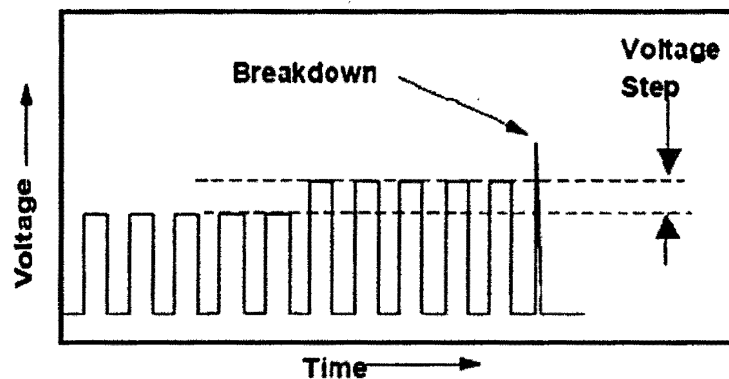


Figure 33. Increasing voltage pulse of SSST test

After the fifth pulse, the voltage setting is incremented slightly, and the next pulse train applies the higher voltage pulses to the capacitor. This five-pulse cycle is repeated at incrementally higher voltage until the capacitor breaks down.

The voltage for the first pulse train is set to ½ of the rated voltage. The final voltage is at 4x of the rated voltage. The step voltage is based on the range from start to stop, to allow a full test to take place within a 15 to 40 step sequence. Step increments of 10% of the rated voltage are selected based on the starting voltage and the range.

The block diagram and the actual testing set up are shown in Figure 34. The power supply is high current, capable of supplying 20 amperes at a constant rate. The input to each capacitor is isolated and buffered with a 5,000-uF-capacitor bank to assure high charge currents. A relay device is used to switch on the current to the individual capacitor, each with a turn-on resistance of less than 20 milliohms. The discharge of the test capacitor is again through a 0.5 ohm resistor.

The voltage at which each capacitor in a sample fails is recorded and the percentage of failures is plotted versus breakdown voltage on a Weibull probability scale. For ease of comparison, the breakdown voltages are normalized with respect to rated voltage.

Figure 35 compares a number of 6.3V rated PA capacitors from 3 different manufacturers (A, D, and C) with a polymer tantalum capacitor made by manufacturer D. The worst SSST breakdown voltage is found to be the 470 µF, rolled foil capacitor made by manufacturer C. The breakdown voltages in this capacitor range from 11.0V to 12.5V or 1.75 to 2.0 times of rated voltage, a range of 1.14:1. Such low values in

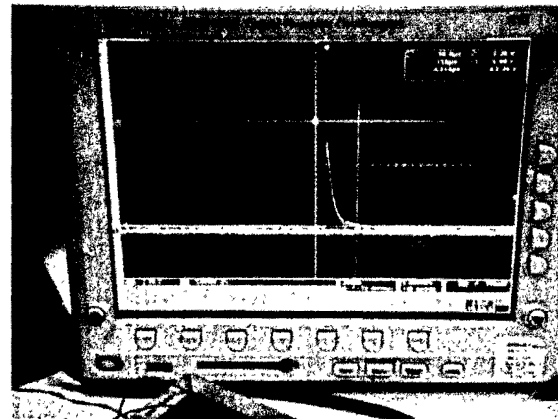
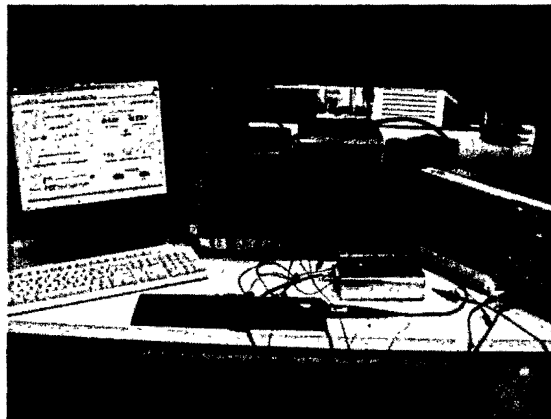
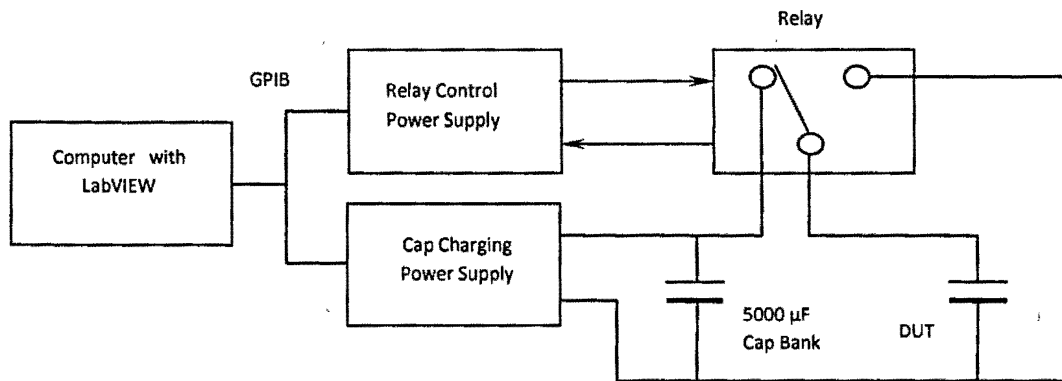


**Figure 34.** Block diagram and actual SSST test set up used in this research.

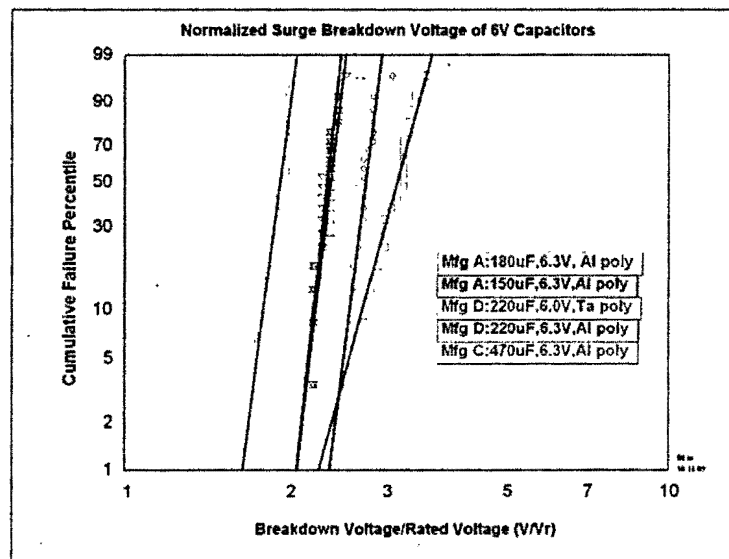


**Figure 35.** Normalized SSST breakdown voltages for 6.3V PA and tantalum polymer capacitors made by different manufacturers.

breakdown voltage suggest that the rolled foil construction is not a compelling technology for the construction of PA capacitors. Other three PA capacitors made by manufacturer A and D show breakdown voltages range from 2.2 to 3.0 times of rated voltage, or a range between 1.14:1 to 1.24:1. The tantalum polymer capacitor made by manufacturer D, shows the highest breakdown voltage in the group, with a range of 2.3 to 3.6 times of rated voltage and a range ratio of 1.54:1. However, the first failure is almost in the same ratio of rated voltage (2.2 versus 2.3 times of the rated voltage) for both PA and Ta-Poly capacitors. In addition, PA capacitors also exhibit a smaller range ratio (1.24 versus 1.54 for Ta cap), indicating a tighter distribution in breakdown voltages.

The breakdown voltages for a 10V, 100  $\mu$ F fused MnO<sub>2</sub> tantalum capacitor and a 12V, 100  $\mu$ F, PA capacitor are shown in Figure 36. The breakdown voltage ranges from 1.8 to 2.6 times of rated voltage for the PA capacitor and 1.4 to 2.7 for the MnO<sub>2</sub>-based tantalum. Again, the PA capacitor also exhibits smaller range ratio of 1.44:1 versus 1.93:1 for tantalum.

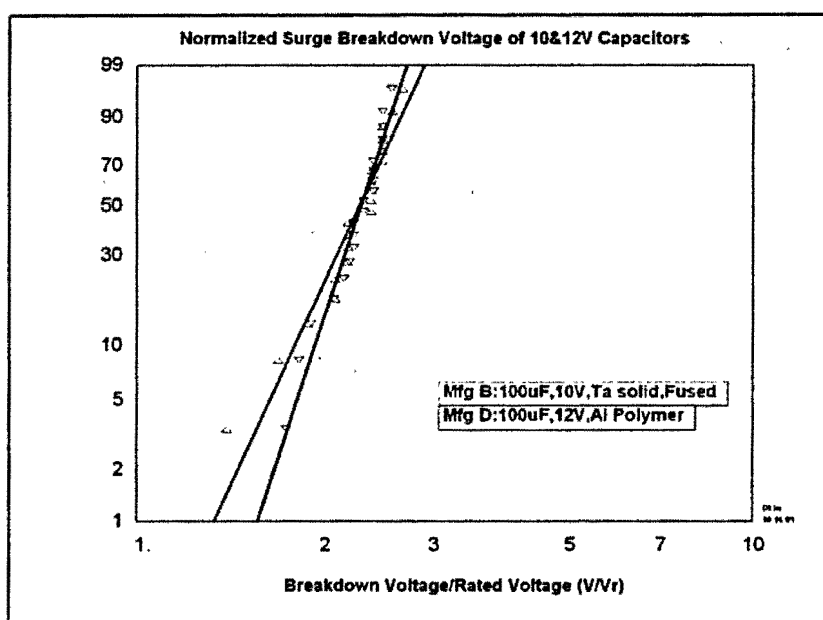


**Figure 36.** Normalized SSST breakdown voltages for 12V, 100  $\mu$ F, PA capacitor made by manufacturer D and for 10V, 100  $\mu$ F, fused MnO<sub>2</sub> tantalum capacitor made by manufacturer B.

The breakdown voltages for 4V and lower rated voltage PA capacitors are shown in Figure 37. A 4V, MnO<sub>2</sub>-based tantalum capacitor is also used for comparison purpose. The breakdown voltage ranges from 2.4 to 3.2 times of rated voltage for the 4V PA capacitor, 3.5 to 4.7 for the 2V PA capacitor, and 2.8 to 6.5 for MnO<sub>2</sub>-based tantalum capacitor. The Weibull probability distribution functions (PDF) for the capacitors are also shown in the bottom plot in Figure 37. This plot clearly shows the distribution tightness of breakdown voltages in PA capacitors. This corresponds to a much lower PPM failure rate at a given percentage of the rated voltage. This suggests that voltage de-rating may not be necessary for these PA capacitors. More thorough analysis of the subject will be continued in FY10 research.

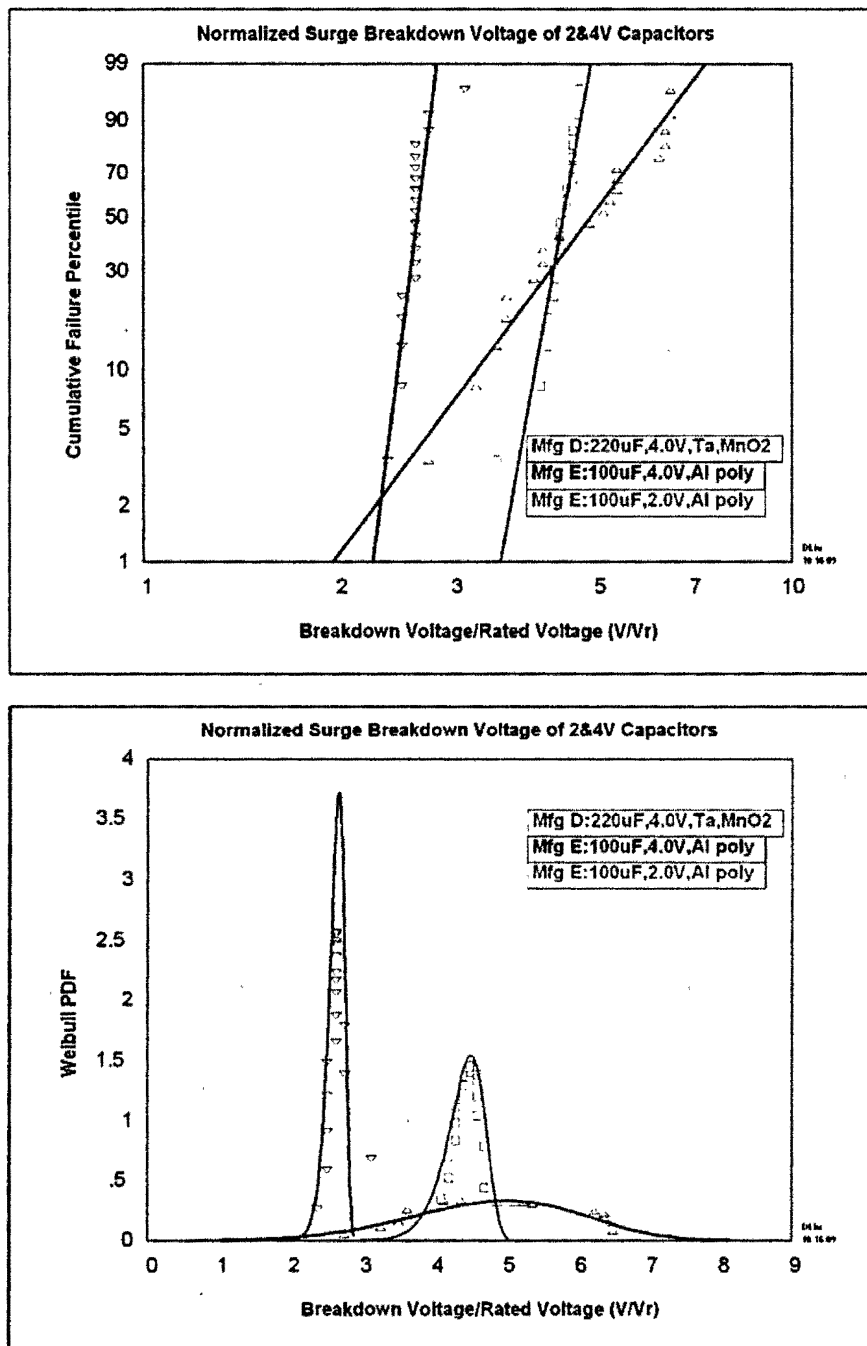


**Figure 37.** Normalized SSST breakdown voltages for 4V and 2V, 100  $\mu$ F PA capacitor made by manufacturer E and for 4V, 220  $\mu$ F, MnO<sub>2</sub>-based tantalum capacitor made by manufacturer D. The Weibull probability distribution function plot (below) clearly shows the tight distribution in breakdown voltage for Pa capacitors.

## Conclusions and Future Work

The results of this initial study on polymer aluminum (PA) capacitors has yield several important conclusions.

1. The physical construction technology of PA capacitors varies with manufacturers, from conventional rolled foil, V-shape stacking, to dual-layer sandwich structure. The electrical characteristics of PA capacitors highly depend on the construction technology. The PA capacitors made with rolled foil technique show high dielectric loss and high DC leakage, lower frequency capacitor roll-off, and lower breakdown voltage. The capacitors with sandwich structure exhibit the best performance in low ESR, high frequency stability, high breakdown voltage and should be considered to replace the  $\text{MnO}_2$ -based tantalum capacitors in this voltage range.
2. PA capacitors demonstrated performance over  $\text{MnO}_2$ -based solid tantalum capacitors and even tantalum polymer capacitors with extremely low ESR and superior stability of capacitance versus frequency and temperature, especially in the low voltage range (6.3V or less).
3. All PA capacitors exhibit ignition-free, non-flammable failure mode when a "push-to-fail" test is performed with substantial amounts of current flow being applied at twice the rated voltage.
4. No impact has been revealed on the electrical performance of PA capacitors before and after thermal vacuum test of 12 cycles, between  $-44^\circ\text{C}$  to  $+105^\circ\text{C}$ , at  $10^{-5}$  Torr.
5. Most PA capacitors demonstrated uniform dielectric breakdown voltage distribution, indicating a lower PPM failure rates at a given operation voltage.
6. As one of the deliverables for this year, a draft outline of a qualification plan for PA capacitors is proposed and as attached in Appendix.

Based on the first year research results, the work for future is proposed into two groups. The first group lists those that were unable to be completed due to the short performance period of FY09 (It actually started on April 1<sup>st</sup>, 2009)

1. Extending frequency-domain electrical testing down to temperatures as low as  $-95^\circ\text{C}$  as previously performed for tantalum polymer capacitors. Therefore, apple-to-apple performance comparison between the polymer Al and Ta capacitors can be revealed completely.
2. Extra numbers of PA capacitors are to be destructively tested for SSST in order to achieve a fairly high level of confidence for the PPM-level failure rate analysis.

The second group of list for future work includes the tests necessary for the completion of this line of work and the applicability of the testing to space qualification of PA capacitors (in priority order).

1. The long term reliability of the PA capacitors such as  $125^\circ\text{C}$  dry life and  $85^\circ\text{C}/85\%\text{RH}$  humidity test shall be performed. This task also includes the hardware construction of a life test setup in modifying the purchased environment chamber that allows a simultaneous testing of 200 capacitors with different rated voltage at various temperatures.
2. Statistical analysis should be performed on the PPM failure rate determination and de-rating criteria establishment for PA capacitors. The time-to-failure analysis is also necessary in order to determine the long-term failure rate and failure model in PA capacitors. This is a critical step to qualify PA capacitors for space applications. Purchase of modeling software is required.
3. Radiation testing should be performed. At this moment, only the total ionizing dose (TID) testing specifications have been planed. The PA capacitors will be tested under load and no load conditions from 100 krad (Si) and gradually go up to 500 krad or even 1,000 krad (1M rad). The testing will be coordinated with Radiation Branch (Code 561) and performed at GSFC campus.
4. High temperature performance of PA capacitors.



**Appendix: Qualification Plan for PA Capacitors (Draft)**

<b>Reliability / Environmental, Physical, Mechanical, and Process Tests</b>		
High Temperature Life	MIL-STD-202, Mthd 108	125°C, Rated Voltage, 2000 Hours
Storage Life Test	MIL-STD-202, Mthd 108	125°C, 0V, 2000 Hours
Load Humidity	MIL-STD-202, Mthd 103	85°C / 85%RH, Rated Voltage, 1000 Hours
Temperature Cycle	JESD22 Mthd 104	Cycle -55°C to +125°C, 1000 Cycles
Thermal Shock	MIL-STD-202, Mthd 107 -	55°C to +125°C, 20s transfer, 15 min dwell, 300 Cycles
Moisture Resistance	MIL-STD-202, Mthd 106	Cycled Temp / RH, 0V, 21 cycle @ 24 Hrs each
Thermal Vacuum Cycling	GSFC-STD-7000	12 cycles at pressure $<10^{-4}$ Torr; -44°C to +105°C
Radiation Test	TBD	TBD
<b>Physical, Mechanical &amp; Process Tests</b>		
External Visual	MIL-STD-883, Mthd 2009	Evaluate physical external character of all parts submitted for test.
Physical Dimensions	JESD22 Method JB100	L, W, and T Dimensions
Destructive Physical Analysis	EIA-469	Electrical test not required.
Terminal Strength	AEC-Q200-006 JIS-C-6429	Force of 1.8 kg for 60 seconds
Resistance to Solvents	MIL-STD-202, Method 215	Include Aqueous wash chemical – OKEM Clean or equivalent
Solderability	ANSI / J-STD-002	a) Method B, 4 hrs @ 155°C dry heat @ 235°C
		b) Method B, category 3, 8 hr steam age @ 215 and 260°C dips
		c) Method D, category 3, Leaching @ 260°C dip
Resistance to Soldering Heat	MIL-STD-202, Mthd 210	Condition B, no pre-heat of samples, Single Wave Solder
Mechanical Shock and Vibration	MIL-STD-202 Mthd 213/214	Method 213: Figure 1, Condition F Method 204: 5gs for 20 min, 12 cycles